FINITE ELEMENT MODELING OF TIRE-TERRAIN DYNAMIC INTERACTION FOR

FULL VEHICLE SIMULATION APPLICATIONS

Shahyar Taheri

Saied Taheri, Chair
Corina Sandu, Co-Chair
Mehdi Ahmadian

May 1st 2014
Blacksburg, Virginia

FINITE ELEMENT MODELING OF TIRE-TERRAIN DYNAMIC INTERACTION FOR FULL VEHICLE SIMULATION APPLICATIONS

Shahyar Taheri

ABSTRACT

Studying the kinetic and kinematics of the rim-tire combination is very important in full vehicle simulations, as well as for the tire design process. Tire maneuvers are either quasi-static, such as steady-state rolling, or dynamic, such as traction and braking. The rolling of the tire over obstacles and potholes and, more generally, over uneven roads are other examples of dynamic events which are of importance. In the latter case, tire dynamic models are used for durability assessment of the vehicle chassis, and should be studied using high fidelity simulation models. In this study, a three-dimensional finite element model (FEM) of the 16 inch TMPT Tire has been developed using the commercial software package ABAQUS. The purpose of this study is to investigate tire transient dynamic behavior for various inputs. The process of running dynamic FE tire simulations starts by statically inflating and loading the tire using an implicit method with refined mesh in the contact patch. Then, by using the "result transfer" option in ABAQUS, final state vectors are used as initial conditions for subsequent simulations. Using this sequence of loading steps helps increase the efficiency of the code. The validation of the model is performed in two stages. First, tire mode shapes and associated natural frequencies and damping values are compared with the experimental data. Second, a series of transient dynamic simulations are performed using an explicit method with a fine mesh around the circumference of the tire. Finally, the FEM model results are filtered to eliminate the numerical noise, and their correlation with the test data is investigated. Moreover, the peak values and time shifts associated with spindle forces as a function of normal load are studied. The results show that the tire dynamic response is autonomous.

ACKNOWLEDGEMENTS

TABLE OF CONTENTS

LIST OF FIGURES

LIST OF TABLES

Chapter 1: Introduction.

1.1 Overview

The tire functions as an interface between the vehicle and the road. The tire air-filled structure can provide a cushion to support the vehicle weight, and filter road irregularities for a smooth ride. Additionally, all forces and moments needed for driving, braking, and cornering are transferred between the vehicle and road through the tire. These forces and moments are generated due to the tire deflection in the corresponding directions. The force generation capacity of the tire is a function of the tire-road contact properties and tire deflection, which in turn is influenced by the tire structural design and material properties. Tire should comply with various design and safety requirements in order to provide safe and reliable performance characteristics for the vehicle and passengers. These performance requirements extend beyond the vehicle/passenger, and impact the environment through waste of energy due to the tire rolling resistance, pollution from the tire manufacturing process, degradation of the road surfaces, and road accidents due to the tire failure.

In order to correctly design and analyze the tire behavior, a precise model of the tire structure should be implemented. This structural model will be augmented with a tire-road interaction model to fully characterize the dynamics of the tire. The integrated package of the tire structural model and tire-terrain interaction model is usually referred as the tire model by researchers. Generally, the tire structural model will be more realistic and accurate if it captures the details of the tire material properties and mechanical structure. Additionally, the accuracy of the tire-road interaction model is directly related to the level of contact patch discretization and the method by which the kinetics and kinematics of the contact phenomenon are captured. The overall process of modeling and analyzing the tire behavior is challenging due to its highly non-linear dynamic characteristics.

These non-linearities exist in the material properties representation of the tire's constituent parts (e.g., rubber and reinforcements), in addition to the partial differential equations that capture tire structural responses such as elastic and plastic interaction between components (e.g., interaction between carcass and belt).

The areas in which a tire model is exploited for analysis can be categorized into two main case studies. The first application is in the early stages of the tire design, in which the choice of the tire structure geometry and material properties is studied, and their effects on various aspects of the tire performance go under extensive analysis. In these simulations, the overall dynamics of the tire in addition to the stresses and strains within the tire structure are investigated to achieve a more reliable and optimized tire design scheme. The second application is in the hybrid simulations in which the tire behavior, and the interaction of the tire with the vehicle are considered simultaneously. The examples for this type include NVH analysis (noise, vibration, and harshness), handling analysis, control applications and etc. The employment of these tire modeling methods from the design stage to development and manufacturing stages, results in a lower total production cost within a shorter time.

Throughout the years, various tire models have been developed, and some of them implemented into commercially available software such as FTire [1]. Selecting an appropriate tire model is based on the targeted area of application in addition to the available computational and experimental resources. There is not a single tire model that can be utilized for studying the tire response under all sorts of loading scenarios and operating conditions. Generally, these models can be grouped into three main categories: 1) Empirical models, 2) physics-based models, and 3) semi-empirical models.

The empirical models use the experimental data of the tire response and correlate it to the influential parameters of the system via mathematical equations. These models are very useful as simple tools for evaluating the performance of the vehicles in conditions similar to the test environment and with tire properties similar to the test tire. Due to this limitation, empirical models cannot be used for extrapolating the results to the problems outside the scope of the experimental tests. Thus, a new tire design concept or a new operating condition for testing the tire performance cannot be studied using this family of tire models. Also, the empirical models developed for passenger and truck size tires do not scale perfectly to the smaller size tires such as tires in robotic applications and lunar vehicles.

Instead of using experimental analysis to characterize the tire-terrain interaction, physics-based models incorporate the physical principles and analytical methods to represent tire structures and tire-terrain interaction. This multi-disciplinary field of models incorporates applied mathematics, numerical analysis, computational physics, and even computer graphics to evaluate the performance of the vehicles. Here, the degree of complexity varies from the simple models that consider tire as a cylinder, membrane, or shell of revolutions to very detailed models that use the finite element formulation for characterizing the tire.

The semi-empirical models combine experimental measurements, empirical formulations and analytical methods to model the tire-terrain interaction. Using such a hybrid approach reduces the computational effort, and simultaneously makes it possible to conduct multiple simulation case studies. This makes the semi-empirical tire models good candidates for full vehicle simulations as well as control applications. However, in those aspects, in which these models incorporate the empirical correlations, the limitations of the empirical models prevail.

Investigating the tire model behavior is typically conducted for two types of tire responses. For the first type, tire steady-state response is studied for the case studies involving out-of-plane cornering factors (e.g., lateral deformation, lateral forces, and self-aligning moments), gradual slip changes, stiffness analysis, etc. The second type focuses on the transient response of the tire in in-plane and out-of-plane maneuvers, such as traction, braking, cleat tests, etc. The tire models, which are capable of capturing the tire transient behavior, should be initially validated for steady-state situations, and, consequently, they could become functional for steady-state case studies, too.

1.2 Objectives.

During the design stage of the tire and car components that are directly influenced by tire behavior, such as suspension, different loading scenarios should be considered. Based on the type of loading inputs and tire boundary conditions, the tire presents a static, quasi-static, steady-state dynamic, or transient dynamic behavior. Among these, due to their impulsive force and moment characteristics, transient responses of the tire are the main focus of this study. The objective of this study is to develop a validated finite element tire model that can be used to study the transient response of the tire due to various dynamic events. This model is validated against the quasi-static and modal analysis test data and is used to investigate the dynamic response of the tire in case studies such as accelerating/decelerating and cleat tests.

1.3 Methodology.

The finite element method is chosen as the framework for modeling the tire nonlinear system. This method allows modeling detailed geometrical and material properties of the tire, which can encompass time and frequency dependent material characteristics. Also, models developed in this manner can easily be adjusted for different boundary conditions and loading scenarios. Incorporating this approach can be a substitute for the physical tire evaluation process, which is

time-consuming and is not cost-effective by nature [2]. Additionally, compared to empirical and semi-empirical tire models for which the accuracy is highly dependent on the parameterization procedures and test conditions, finite element models (FEM), once parameterized using geometrical and material properties, can be used in a wide variety of testing conditions [3].

This finite element model is used for studying the tire transient dynamic behavior for dynamic maneuvers such as traction, braking, and cleat negotiation. The importance of this research is that it considers a detailed FEM model for the tire sections, which includes different tire hyper-elastic, viscoelastic, and elastic material properties. Additionally, a hybrid explicit/implicit approach is developed to reach the final dynamic results more efficiently. More importantly, the experimental modal analysis and cleat test data are used to assess the validity of the developed FEM tire model.

The tire used in this study is a Michelin 205/55 R16 90, from the Tyre Model Performance Test (TMPT) program. A hybrid implicit/explicit approach is chosen to assure model convergence. This method uses an implicit approach for initial stages, such as inflating, loading, and steady-state rolling of the tire. This makes the run time for reaching the transient simulation initial conditions, such as tire velocity, independent of the initial conditions. Therefore, at the end of the steady-state stage, the final state-vector of the tire elements, which is the output of the model state-space solver and contains nodal information such as position, velocity, and forces, is used as the initial condition for transient simulation.

To verify the model under steady-state conditions, modal analysis test is conducted, in which tire mode shapes, natural frequencies and damping values are extracted and are compared to the simulation results. As for tire dynamic behavior, a series of transient maneuvers are performed to study the dynamic response of the tire. In these tests the tire forces generated using the developed

5

FE model are compared with the experimental data for validation purposes. Additionally, the effect

of the loading on spindle force properties is evaluated in details.

The methodology of the proposed work is presented in Figure 1.
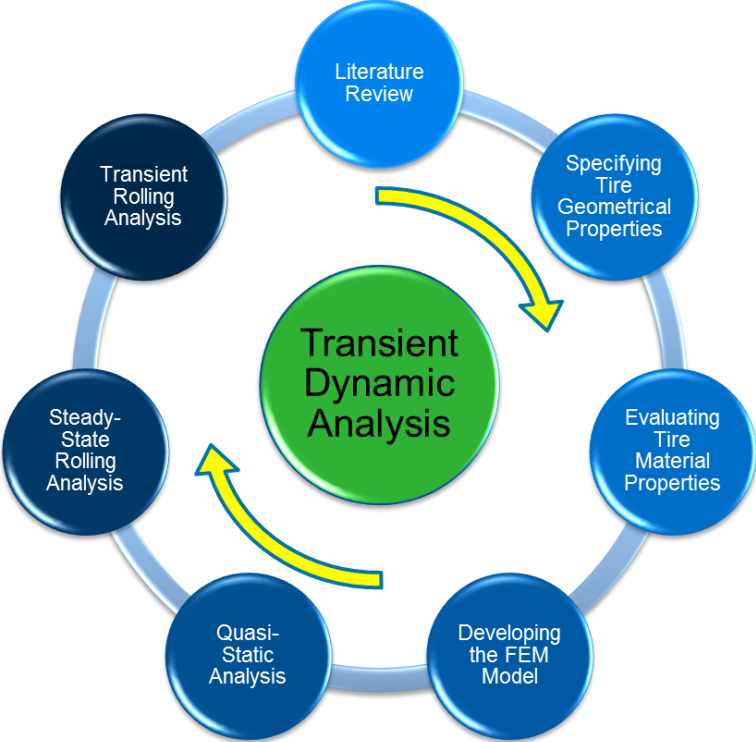
Figure 1: Methodology of the proposed work

Chapter 2: Literature Survey

2.1 Introduction

The complexity of the tire models has evolved throughout the time; new modeling techniques and more powerful computational tools are continuously being developed and introduced. The simpler models represent the tire structure using a lumped parameter approach that discretizes the tire belt into an elastic ring, string or beam, suspended on an elastic/plastic foundation. These models require tests to identify the equivalent lumped properties of the system. This procedure is highly dependent on the discretization level of the system in addition to the type of force elements that are used between the system components. Additionally, these models, due to their simplified approach, lack some of the system informative factors, such as precise local deformation of the contact patch and complete response spectrum of the system (e.g., frequency content of the response).

The more detailed tire models that incorporate finite element methodology to discretize the tire structure to a higher extend are considered to be more complex. For parameterizing the FEM tire models, one needs to conduct the experimental tests to fully define the material models to be used in the code. Once the material models are fully defined, they can be used in various design configurations without the need to characterize the system again, similar to the lumped parameter approaches. All of these come at the cost of more tedious modeling effort and higher computational time. In addition to the aforementioned models, there are some semi-analytical, semi-finite-element models that consider some simplification of the actual problem or incorporate the tire experimental data in order to fully explain the tire mechanics with less computational effort.

In this section, the methodologies, challenges, and perspectives of developing a tire model for the vehicle simulations are documented. First, the influential forces and moments in studying the tire behavior are identified and an appropriate coordinate system is introduced. Then, the mechanics of the tire-terrain interactions that lead to generation of these forces and moments, at the interface of the tire with ground (known as contact patch), are studied. Subsequently, the methodologies for developing a framework for modeling and simulation of the tire structural behavior and tire-road interaction are reviewed. Moreover, the experimental procedures for model parameterization and validating the model output responses are reviewed. Finally, an overview is given for constructing the interface between the tire model and the multi-body dynamic software. Through this interface, tire model can communicate with the vehicle model and function as a tire-ground interaction module in the vehicle simulation.

2.2. Tire Force and Moments

In order to identify forces and moments that are generated in the contact patch of the tire, we first need to specify a coordinate system that serves as a reference. The Society of Automotive Engineers (SAE) has introduced an axis system as shown in Figure 2 [4].
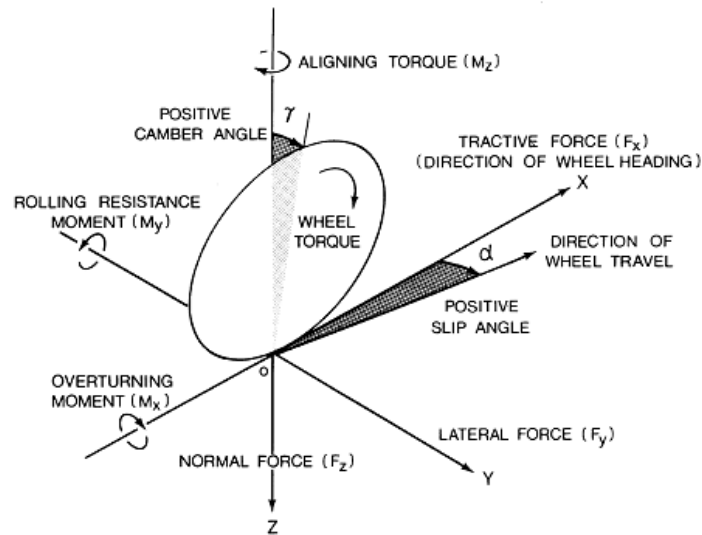
Figure 2: Tire coordinate system by SAE (Theory of Ground Vehicles, 4th ed., Wong, J.Y., 2008, Hoboken, NJ, used with the permission of John Wiley & Sons, 2014)

The origin of this coordinate system is located at the center of the contact patch. The Z axis points downward and is perpendicular to the ground plane. The X axis is the interaction of the ground plane and wheel plane with the positive direction pointed to the direction of motion. Finally, the Y-axis direction is chosen in such a way that makes the coordinate system orthogonal, and as a result, it is located in the ground plane and points to the right of the wheel plane.

The forces and moments are generated along, and respectively about, all axes directions during the operation of the tire. These forces and moments are caused by the interaction of the tire with the road surface (e.g., driving, braking, cornering, and road irregularities), and suspension inputs (e.g., sprung mass weight, reaction and inertia forces). The applied forces to the tire are: 1) F_x: tractive force or longitudinal force, 2) F_y: lateral force, 3) F_z: vertical force. The moments are: 1) M_x: overturning moment, 2) M_y: rolling resistance moment, 3) M_z: aligning moment. Using this coordinate system, we can define the performance parameters of the tire conveniently. For example, the traction/braking force is calculated by integrating the longitudinal shear stress over

the tire contact patch. Additionally, the driving/braking torque over the tire's axis of rotation produces a force for accelerating/decelerating the vehicle. The mechanics involved in generation of the tire forces may come from different sources. For instance, the tire longitudinal forces are a resultant of tire rolling resistance force, longitudinal friction force, and longitudinal reaction force. In the following sections, the tire stiffness due to the loading is defined first, and then the description for the tire major force and moment components, in addition to the physics behind their action, are given.

2.2.1 Tire stiffness

The tire shows a hyper-elastic behavior in compression and tension loadings. In a hyper-elastic material, the stiffness is different in compression and tension. The tire deformation characteristics, due to the applied forces in longitudinal, vertical, and lateral directions, are very important in tire dynamics. In order to specify the loading-deformation dependency, usually, an experimental analysis is carried out. The results from such an experiment are represented as stiffness curves, such as shown in Figure 3. It can be seen that these curves deviate from the linear regime with an increase in loading. This behavior originates from the nonlinearities in the tire structure, such as internal hysteresis, as well as tire-terrain interactions. The tire forces in different directions are functions of the deflection magnitude and the deflection velocity. The slope of the experimental curves at each deflection point is called the tire local stiffness. In a certain direction, the tire stiffness tangential value at zero deflection is called the linear stiffness coefficient. The tire linear stiffness coefficients are used for the vehicle dynamic analysis and control applications.

10
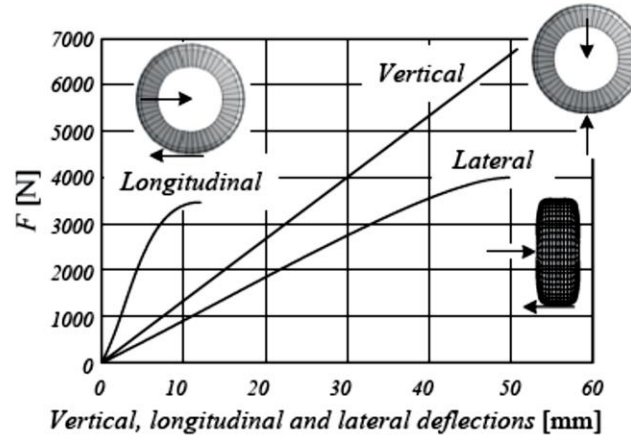
Figure 3: Vertical, longitudinal, and lateral stiffness curves (Vehicle Dynamics: Theory and Application, Jazar, R.N., 2008, used with kind permission from Springer Science and Business Media)

2.2.2 Tire longitudinal force: rolling resistance

Rolling resistance is the negative force, which is generated due to the rotation of the tire. The physical scheme of this force is based on multiple phenomena. During the rolling of the tire on a surface, the tire carcass repeatedly goes under deflection. Due to the hysteresis in the tire materials, the loading-unloading process of the tire structure dissipates energy. This energy loss accounts for a part of the rolling resistance on the tire. The circulation of the air inside the tire chamber and the flow of the air over the tire are other factors that impose drag forces on the tire. Additionally, during the traction/braking phase, the normal stress distribution in the contact patch shifts forward/backward relative to the tire YZ plane. Consequently, the resultant normal force from the ground will produce a negative/positive moment around the Y axis that resist the accelerating/decelerating. Some studies [5, 6] have shown that in the speed range of 80-95 mph, the proportion of the rolling resistance force components are as follow: 90-95 % from the internal hysteresis losses, 2-10 % from the tire-terrain interaction friction, and 1.5-3.5 % from the air resistance.

11

The rolling resistance is a function of tire design and material properties, in addition to the operational factors, such as normal load, speed, temperature, inflation pressure, and road surface. The radial tires, due to their superior contact patch stress distribution, tend to have a lower rolling resistance coefficient as compared to the bias ply tires, as shown in Figure 4 [7]. Increasing the thickness of the sidewall or tread, number of tire plies, and the amount of the synthetic rubber (instead of natural rubber) in the tire structure, can intensify the energy loss in the tire [8]. Also, the rolling resistance of the tire is higher at higher normal loads, higher vehicle speeds, lower inflation pressure, and lower operational temperature.
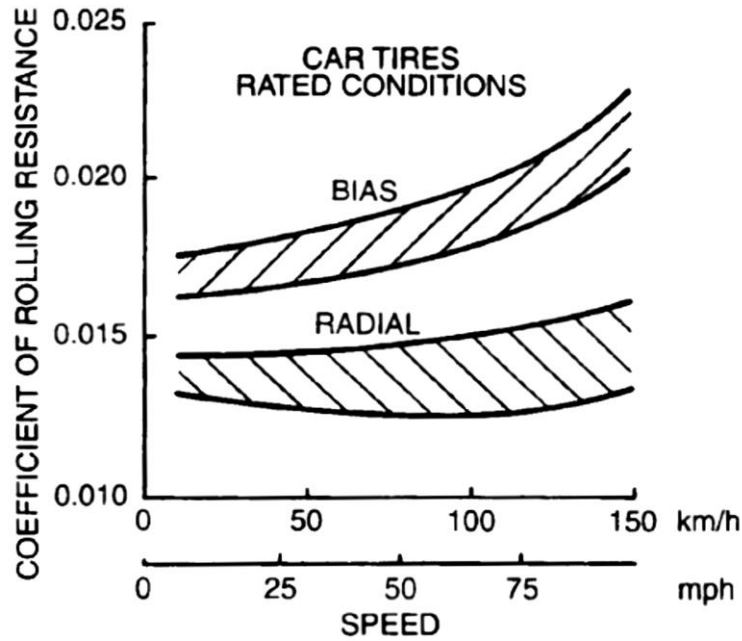
Figure 4: Variation of the rolling resistance values for radial and bias tires at different rolling speeds (Theory of Ground Vehicles, 4th ed., Wong, J.Y., 2008, Hoboken, NJ, used with the permission of John Wiley & Sons, 2014)

The ratio of the rolling resistance force to the tire normal load is defined as the rolling resistance coefficient. The rolling resistance coefficient varies with the deformability and texture of the surface. This value is significantly higher for terrains with soft texture and high surface roughness. Also, the wet surfaces usually show higher rolling resistance compared to dry surfaces. It should

be noted that the characterization of tire rolling resistance, due to its complex nature, relies mostly on experimental procedures. The SAE handbook of Society of Automotive Engineers introduced an experimental procedure for measuring this parameter and formulating it through empirical correlations [reference].

2.2.3 Tire longitudinal force: frictional force

The acceleration and deceleration of a tire is based on the generated frictional force at the contact patch. When a driving/braking torque is applied to the tire, it compresses/stretches the tread elements prior their entrance to the contact patch. Due to this shear deformation, a longitudinal shear stress distribution is generated at the contact patch. This scenario is often referred to as the longitudinal slip, which is caused by the elastic deformation of the tire tread. As a result, the distance that a tire travels when a driving/braking torque is applied is less/more than in the free rolling condition. The longitudinal slip ratio based on the direction of the applied torque is defined as:

- For driving torque: $slip\ ratio\ (\%) = \left(1 - \frac{V}{r\omega}\right) \times 100 = \left(1 - \frac{r_e}{r}\right) \times 100$

- For braking torque: $slip\ ratio\ (\%) = \left(1 - \frac{r\omega}{V}\right) \times 100 = \left(1 - \frac{r}{r_e}\right) \times 100$

Where V is the tire speed, r is the radius of the free rolling tire, r_e is the radius of effective rolling tire, and ω is the tire angular velocity. The effective rolling radius of the tire is the ratio of the tire speed to tire angular velocity. Using these definitions, the sliding of the tire can be expressed as the driving/braking situations in which the slip ratio is 100 %. This will happen when a high driving/braking torque is applied to the tire on a low friction surface such as ice. The available coefficient of friction from the ground is highly dependent on the slip ratio. Usually, the peak of

this coefficient is located at around 10-30 % slip ratio range, which is the domain in which the anti-skid brake systems (ABS) attempt to operate, as seen in Figure 5 [4].
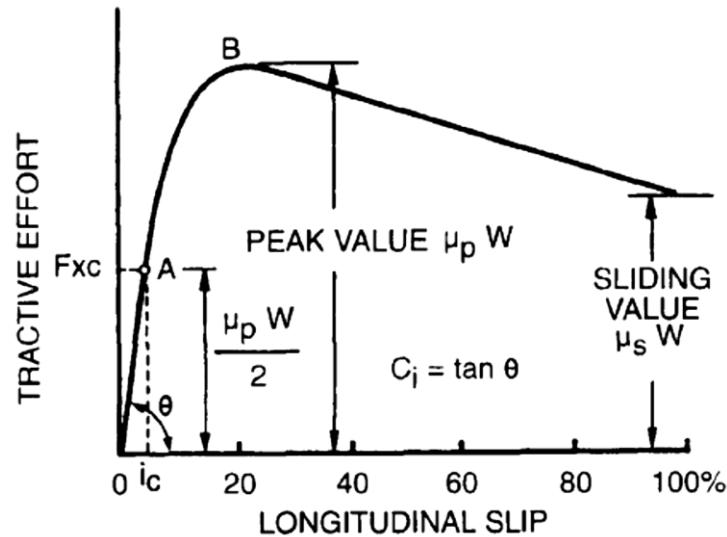
Figure 5: The tractive force dependency to longitudinal slip ratio (Theory of Ground Vehicles, 4th ed., Wong, J.Y., 2008, Hoboken, NJ, used with the permission of John Wiley & Sons, 2014)

It is worth mentioning that SAE [9] uses a different definition of the slip ratio than what is presented here. In this definition, slip ratio is defined as "the ratio of the longitudinal slip velocity to the spin velocity of the straight free-rolling tire expressed as a percentage", and the longitudinal slip velocity is expressed as "the difference between the spin velocity of the driven or braked tire and the spin velocity of the straight free-rolling tire". A detailed description of the mechanism involved in generating the friction force is given in section 2.3.1 Tire-terrain friction.

2.2.4 Tire longitudinal force: reaction force

The longitudinal reaction force is the longitudinal component of the reaction force applied to the tire while traveling over the road irregularities such as speed bumps, steps, ditches, and path holes. When the tire encounters these obstacles, a sudden deformation is imposed on its structure due the changing road boundary condition. This abrupt input results in a three dimensional opposing tire

force, which is transmitted to the suspension, and can cause damages to the wheel assembly, and vehicle suspension. The amplitude of this force is a function of obstacle geometry, suspension properties, vehicle load, speed, and inflation pressure.

2.2.5 Tire lateral force and aligning moment

The lateral force is generated at the tire contact patch when the vehicle is subjected to a cross wind or it undertakes a cornering maneuver. In order to initiate a cornering maneuver, an input moment around the z-axis is applied to the tire, which produces an angle α between the wheel plane direction u and direction of travel v', as seen in Figure 6. The angle α is usually referred to as the tire slip angle. This angular difference causes the deflection of the tire plies, and consequently production of the lateral force, known as cornering force. The direction of this force is headed toward the instantaneous center of rotation for the related wheel. The cornering force is directly related to the slip angle and the normal load on the tire, and increases with increasing these factors. It should be mentioned that wide tires, due to their greater contact patch area, have a higher lateral force capacity for the same normal load and slip angel compare to narrow tires.
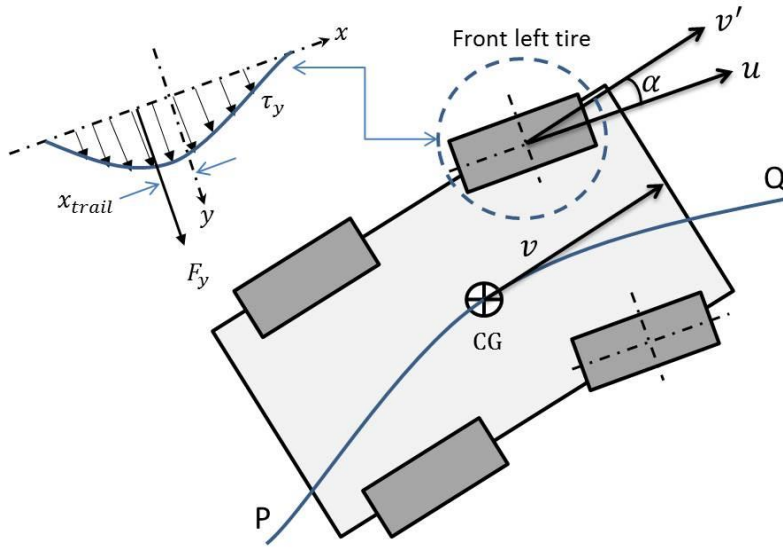
Figure 6: Cornering maneuver with slip angle α (Top view)

The growth in the lateral force generation is limited by the kinetic coefficient of friction between the tire and the road. Generally, the friction force generation capacity in the tire-road interaction is represented as the friction circle, as illustrated in Figure 7. The radius of this circle is the asymptotic value of the maximum friction force, and the resultant force vector (from longitudinal and lateral force vectors) falls within this circle. As a result, accelerating/decelerating longitudinally limits the lateral cornering performance of the tire and vice versa.
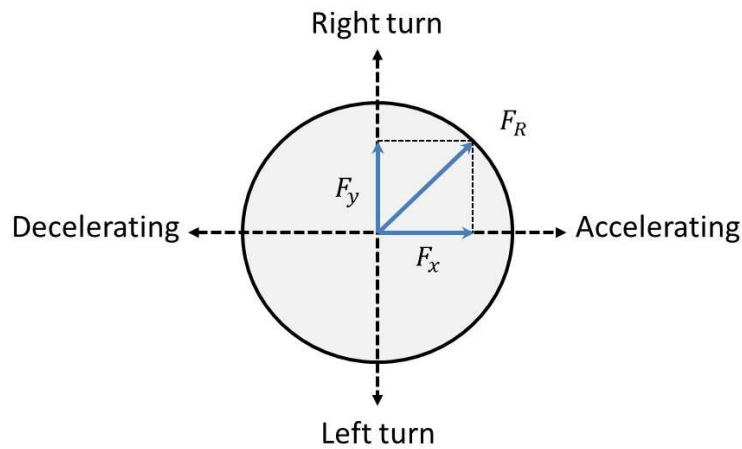
Figure 7: Friction circle

16

By having a closer look at the tire contact patch during cornering, two regions of sticking and

sliding can be identified. As the tire moves forward, the tread elements enter the contact patch and

deflect laterally and longitudinally. This entry region of the tire is called sticking region or

adhesion region, as presented in Figure 8 [5]. As the tread elements proceed to enter in the contact

patch, their distortion, compared to the initial condition, increases, and it will eventually exceed

the available local friction limit of the road. At this point, which is known as the sliding line, the

tread elements start sliding on the road surface. By increasing the slip angle, the adhesion region

in the contact patch dwindles and sliding region grows over the entire contact patch [10].
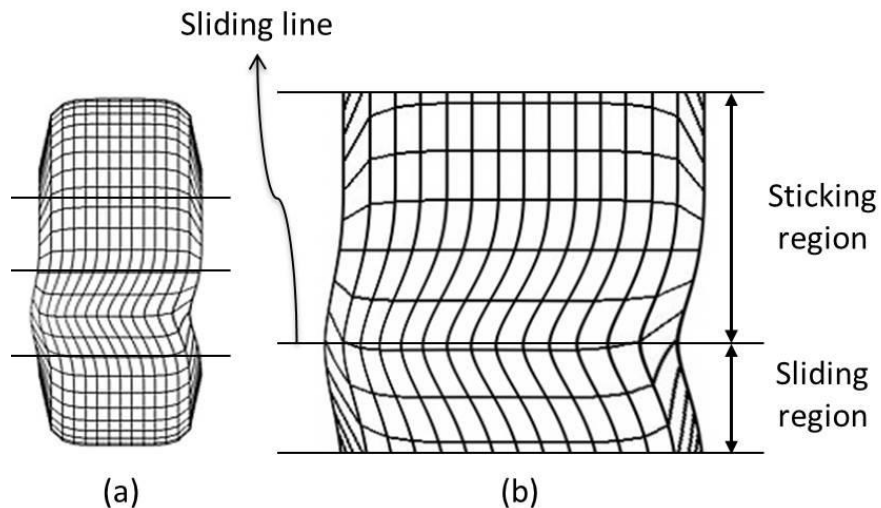
Figure 8: Tire deflection during cornering, (a) bottom view, and (b) magnified contact patch (Vehicle Dynamics: Theory and Application, Jazar, R.N., 2008, used with kind permission from Springer Science and Business Media)

During cornering, a shear stress distribution is generated at the tire contact patch. This stress

distribution is not symmetrical about the YZ plane of the wheel coordinate system. This shifts the

resultant lateral forces toward the tailing edge of the tire with a distance x_{trail} as shown in Figure

6. This distance is called the pneumatic trail, and generates a moment around the wheel Z axis,

known as the aligning moment. This moment tries to align the direction of the wheel with the

direction of the motion. Similar to the lateral force, the aligning moment increases with an increase in the slip angle until it reaches a peak value (approximately in $4°$-$6°$ range), and then it drops to an asymptotic sliding value. This reduction after the peak value is caused by the growing sliding region that reduces the lateral force and the pneumatic trail simultaneously.

2.2.6 Tire vertical force and overturning moment

The applied vertical force on the tire has static and dynamic components. The static part comes from the dead weight of vehicle sprung and unsprung masses. The dynamic part is due to the vertical acceleration of the suspension system, and can grow up to three times higher than the static vertical force. In this regards, due to the fact that the sprung mass is heavier than the unsprung mass, its dynamic effect is more intense. The normal stress distribution, due to the vertical force on the tire, has a symmetrical distribution around YZ plane for the stationary tire. As it was mentioned previously (see section 2.2.2 Tire longitudinal force: rolling resistance), when the tire starts rolling the resultant vertical force, which is calculated by integrating the normal stress distribution over the contact patch, shifts toward leading edge. In other words, the leading and trailing edges of the tire go under compression and extension respectively. This offset produces a moment around the axis of rotation Y, which is called rolling resistance moment.

Furthermore, when the wheel camber angle is zero, the contact patch pressure distribution is symmetrical around XZ plane, and it has a higher value under the sidewall and the center line of the tire due to the higher local vertical stiffness. In case of a camber angle present, the resultant vertical force will offset relative to the XZ plane. This shift along with the vertical force produces an overturning moment around the X axis. When the normal force is coupled with the lateral force, it can magnify the overturning moment. In this case, the overturning moment is intensified with an increase in the normal load, camber angle, and slip angle.

18

2.3. Tire-Road Interaction

Studying the mechanics of the tire-terrain interaction is fundamentally important in characterizing the performance of the tire on terrain. In this regard, the mechanics of the tire-terrain interaction is divided into on-road and off-road case studies. For the on-road studies, the terrain is considered as a solid (non-deformable) surface, and with irregularities. For this type of terrain, researchers have developed various high-fidelity models that can capture the tire response properties [11-14]. Additionally, multiple commercial tire models have been developed for integration with vehicle simulation programs [1, 15, 16]. For off-road cases, the terrain is assumed as a deformable media, and, as a result, the complexity of the contact modeling problem increases.

A direct application of an on-road tire model to simulate tire performance on a deformable terrain is not possible. This is due to the fact that traveling on deformable terrains raises issues for which on-road tire models do not account for. Moreover, the kinetics and kinematics of the tire on deformable terrains are subjected to different design and operational factors, as well as field characteristics. These factors, in addition to the uncertainties that exist in their parameterization, make the formulation of tire-terrain interaction a highly complex problem. Similar to on-road tire mechanics, these methods ranged from very simple empirical methods to highly complex finite element methods.

The interaction of a wheeled vehicle with the ground results in the normal and tangential stress fields in the contact patch of the tire. The integration of contact patch stresses in vertical and longitudinal directions produces resultant ground forces and moments. These forces and moments are related to the operational parameters, like slip ratio, slip angle, normal load, and inflation pressure. Additionally, contact patch stress fields result in geometrical and mechanical changes in the tire. The geometrical changes include tire belt and sidewall deformation, and the mechanical

changes include variation of the tire structural stiffness and damping properties. Therefore, the tire-terrain interaction physics should be characterized initially for simulating the behavior of the tire-terrain interactions in on-road conditions. The main challenge in this regard is identifying and formulating the stress fields in the tire-terrain contact patch. These stress fields are influenced by kinetics and kinematics of both the tire and the terrain. The comprehensive characterization of this interaction requires detailed modeling of both the tire and the terrain. Most tire models that are investigated for this survey consider some preliminary assumptions in order to simplify this interaction. These simplifications are based on the application of the model and require computational and experimental resources.

2.3.1 Tire-terrain friction

The friction between the tire and terrain, which is caused by their relative slip, is the main force for the tire. Notice that the rolling resistance is generated during the tire rotation, while the friction is generated when there is slip between the tire and the terrain during acceleration/deceleration. Although the friction force is generated in the direction of acceleration/deceleration, the rolling resistance is always exerted against the travel direction [17]. The three major physical mechanisms that contribute to the friction production are: adhesion, deformation, and wear/tearing. These friction force components are shown in Figure 9.
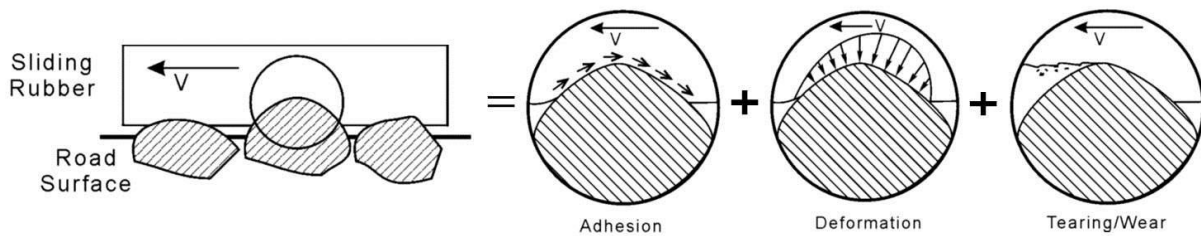
Figure 9: Major mechanisms involved in generation of the friction between rubber and terrain

20

The adhesive characteristics of the tire are due to the Van der Waals intermolecular bonds between two surfaces. The adhesion is considered as the main contribution to the friction force. The magnitude of the adhesion force depends on the contact patch area, which, in turn, is a function of the contact pressure, surface geometry, and material properties. The surface geometry is referred to as the molecular roughness between the contacting surfaces. The friction due to the surface geometry can be reduced by adding some contaminating material to the interfacing surfaces, such as coating, dust, or water.

Other force mechanism in friction generation is due to the rubber deformation, also called mechanical keying. As the tire surface slides over the road surface, the peaks of road irregularities, called asperities, penetrate into the rubber surface. When rubber molecules drape over these asperities, a negative stress distribution is generated at multiple contact regions that ultimately increases the negative friction force. On wet surfaces, the adhesion component of the friction force is reduced and the deformation component provides the main friction between the tire and the road. It should be mentioned that the adhesion and the deformation mechanisms are highly viscoelastic, and their force generation capacity is a function of road profile, sliding speed, and penetration speed.

In addition to adhesion and deformation, the tearing of the rubber inner molecular bonds contributes to tire friction. When the sliding velocity of the rubber increases, at the location of sharp road asperities, the local stresses in the rubber grow. When the local stresses exceed the yield strength of the rubber, the internal polymer bonds and crosslinks fail, and the tire structure deforms beyond the point of elastic recovery. This failure scheme absorbs energy, which is interpreted as an additional component of the surface friction force. Moreover, when the stresses remain high for a long period of time or they exceed far beyond the tearing point, the separation of rubber material

occurs. The tire marks on the road surface, which are produced due to sever acceleration/deceleration of the tire, are caused by tire tearing.

2.4. Tire Modeling Methods

This section gives an overview of the tire models that are developed for on-road simulation applications. As it was mentioned earlier, the main challenge in studying the behavior of the vehicle in on-road conditions is simultaneously characterizing the tire structural response and the tire-terrain interaction. Throughout the years, a wide variety of models have been developed for formulating and simulating this combined problem. The degree of complexity for these models is based on the application, accuracy and computational cost of development. Generally, these models can be grouped into three main categories: 1) empirical models, 2) semi-empirical models, and 3) physics-based models. In this study, a review the most relevant models in each category is performed, with a brief description of the proposed method, its capabilities, and its limitations. As a meter of fact, this survey solely compares the methodologies used by different authors and for more detailed information about the modeling and experimental aspects, the reader should refer to the original texts.

2.4.1 Empirical models

The empirical models use the experimental data of the tire response, and correlate it to the influential parameters of the system via mathematical equations. One of the most famous empirical models is the Magic Formula Tire Model, presented by Pacejka [11]. This model is based on the tire steady-state response data, and relates the tire forces and moments to wheel pure slip values. As a matter of fact, the model includes the dependency of longitudinal force to wheel slip ratio, as well as the lateral force and aligning moment to wheel slip angle. Magic Formula model includes some empirical equations to account for the pressure and temperature effects. Linder [18]

conducted some parametric study and sensitivity analysis on the magic formula in order to evaluate the effect of the model parameters variations to the response of the whole vehicle. He also extended this tire model for case studies that include tire transient response behavior in lateral direction. Later, Apetaur [19] used the magic formula formulation, and added some filters to the model input in order to explain the relations for nonlinear in-plane and out-of-plane tire transient responses. This method assumes that the tire transient forces can be calculated using the tire deformation and related steady-state responses.

Unfortunately, empirical models such as Magic Formula, does not provide a physical meaning of the parameters they are using. This makes it difficult to understand the direct effect of the model parameters changes on physical behavior of the system. Additionally, numerous test iterations should be performed in order to provide enough information in the domain of study for predicting the tire force characteristics. This data should then be curve-fitted to the model equations to find the corresponding model coefficients. As a result, new errors will be introduced in model predictions. Despite all of these drawbacks, this tire model is widely used in industry due to its simple, fast, and relatively accurate (in the domain of derivation) functionality.

Empirical models are very useful as simple tools for evaluating the performance of the vehicles in conditions similar to the test environment and with tire properties similar to the test tire. Due to this limitation, empirical models cannot be used for extrapolating the results to the problems outside the scope of the experimental tests. Thus, a new tire design concept or a new operating condition for testing the tire performance cannot be studied using this family of tire models. Also, the empirical models developed for passenger and truck size tires do not scale perfectly to the smaller size tires such as tires in robotic applications and lunar vehicles. Furthermore, empirical

23

tire models require several sets of data for their parameter estimation process that increases the cost of experimental procedure.

2.4.2 Physic-based models

Instead of using experimental analysis to characterize the tire-road interaction, physics-based models incorporate the physical principles and analytical methods to represent tire and terrain structures, in addition to their interaction. This multi-disciplinary field of models incorporates applied mathematics, numerical analysis, computational physics, and even computer graphics to evaluate the performance of wheeled vehicles. The degree of complexity varies from the simple models that consider the tire as a rigid ring and the terrain as a spring-damper system, to very detailed models that use finite element formulations for both the tire and the terrain.

A tire on road is constantly excited by road unevenness with short and long wavelengths. Consequently, it operates as a filter over the road roughness. Capturing the tire-road interaction for road inputs with high frequency (short wavelengths), compare to the size of the contact patch, is more complex. The tire response at the spindle of the tire is usually smoother than the shape of the obstacle. This behavior has two main reasons; first, when the tire travels over an obstacle, such as a cleat, the forehead of the tire touches the obstacle before the wheel center. Therefore, the distance that tire travels while interacting with an obstacle is longer than the length of the obstacle. Second, the tire has some flexibility at its contact patch, which almost swallows the small irregularities during the enveloping process [20]. Capturing this filtering performance is the main motive for several physic-based tire models. In this regard, Figure 10 shows some of the main physic-based tire models that can serve this purpose. This figure solely provides a 2D illustration of the related models, and some more sophisticated versions of these models include the full 3D contact model.

24
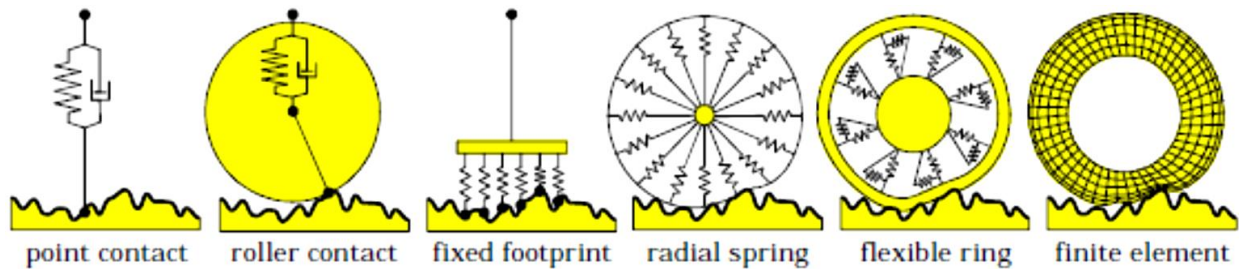
Figure 10: Two dimensional representation of the physics-based tire models that can capture road unevenness

The point contact model is represented by a parallel spring and damper (linear or nonlinear), and is widely used especially in ride analysis. The domain of applicability for this model is long wavelengths, and gradual slopes [20]. Thus, it cannot be used for discrete obstacles, such as cleats, because it will result in high acceleration inputs. The roller contact model uses a rigid disk for enveloping over the road irregularities. The contact is considered only at one point, which is not restricted to be under the wheel center [21]. Using this superior configuration compare to point contact, the high frequency irregularities are filtered out [22]. The fixed footprint model is a parallel combination of the point contact elements attached to a fixed length horizontal bar. This configuration averages the road inputs and transfers a smoother excitation from the road to the vehicle suspension.

The radial spring model arranges a series of linear (or nonlinear) springs in a circular pattern. This model can have multiple contact point based on the road profile. The deflection of each spring is a function of the road height at the associated contact point, and adjacent springs deflection for more advanced models [23]. Gillespie [24] developed a simple radial spring tire model to investigate the effect of the stiffness variation in tire force and moment behavior. He concluded that the magnitude of the radial force changes, from non-uniformities in radial stiffness, is independent of the tire speed. However, the frequency content was shown to be dependent to speed.

25

A more advanced version of radial spring model can be constructed by assigning some point masses at the tip of the radial springs, and considering translational and rotational springs between these point masses and rim as well among neighbor point masses. This model was constructed by Eichler [25] for vibrational analysis of the tires in ride comfort simulations. For validation, he conducted dynamic simulations such as cleat test and pothole test, and compared the model response quantities with experimental data.

The flexible ring model consists of an elastic beam, which is suspended on an elastic foundation. The elastic foundation is a distributed system of spring-damper combinations in radial and tangential directions. As it was discussed in section 2.2.5, the tire vertical stiffness is higher the edges of the contact patch compare to the central region. This behavior is captured in the elastic ring model by the bending of the tread-band. Loo [26] developed a flexible ring tire model in order to predict the vertical loading and rolling resistance characteristics of the tire. For simplification, he neglected the inertia and flexural rigidity of the ring, and parameterized the model inputs experimentally using static point-load tests and contact patch length measurements. For this model, the interaction of the tire with the smooth hard surface is developed using the theory of the elastically supported string.

Finally, the more detailed representation of the tire structure using FEM is described in section 2.4.1.1. Most of the physics-based models conduct experiments in order to parameterize the lumped parameters or material models that they use for modeling the tire structure, terrain structure, and tire-terrain interaction. However, these models usually do not incorporate the empirical formulations for modeling purposes. The lumped parameter physics-based models that assume the concentrated masses or translational/rotational springs and dampers among the model

elements require extensive tests in order to evaluate the equivalent lumped properties. Also, the majority of the models in this group only study the in-plane response of the tire.

It should be noted that the majority of the physics-based models, and especially those that use FEM, have high computational time requirements. The lumped parameter models reduce the degree-of-freedom in the model in favor of the computational effort, which will sacrifice the model accuracy, especially in dynamic transient case studies. Furthermore, different physics-based models consider different approaches for discretizing the tire section, and, consequently, have different parameter inputs. In order to compare the computational speed of the models in this group, similar case studies with the same tire and terrain input parameters should be simulated on the identical hardware platforms.

2.4.1.1 Tire finite element models

Mechanical behavior of the tire and tire-terrain depends on many aspects, such as tire geometrical and material properties, in addition terrain texture and frictional characteristics. Identifying all of these parameters and correlating them to the vehicle performance using empirical closed-form formulations are limited to the similar test conditions. On the other hand, using the simple physics-based methods to model the terrain can lead to significant errors in both estimating model input parameters and capturing terrain mechanics. This will ultimately cause the vehicle response to deviate from experimental data. One alternative numerical method for analyzing vehicle performance is the finite element method. Thanks to the fast rate of computational power improvements, and advancements in developing more sophisticated material models, FEM has become one of the practical tools for analysis of the complex systems.

The assessment of tire transient behavior using FEM has been conducted by many researchers. Due to the limited computational resources, most of FEM tire models developed before 90's are two-dimensional models. In order to study the dissipated energy due to rolling resistance, Padovan [27] used a two-dimensional (2D) curved axisymmetric thin shell element model, and compared the rolling standing wave and tire-road interaction thermal resistance with the experimental data. Similarly, Trivisonno [28] investigated the transient thermal characteristics of the tire using a 2D thin shell elements FEM model. Noor [29] proposed a computational framework for studying three quasi-symmetric tire case studies, which are: (1) linear analysis of anisotropic tires through the use of semi-analytic finite elements, (2) nonlinear analysis of anisotropic tires through the use of two-dimensional shell finite elements, and (3) nonlinear analysis of orthotropic tires subjected to unsymmetrical loading. As an efficient computational approach, this framework assumes an approximation of the unsymmetrical response of the tire with a linear combination of symmetric and anti-symmetric global approximation vectors (or modes). Additionally, Mousseau [30] developed a simple 2D membrane tire model to predict spindle forces during impacting large obstacles.

The study of the tire forces For analysis of flexible pavements that are subjected to dynamic loads, Zaghoul [31] introduced a 3D model in ABAQUS, and validated the model using static and dynamic case studies data. The effect of the tire vibrations, induced by road irregularities, on the vehicle comfort quality was studied by Scavuzzo [32] using a experimentally validated model. Zachow [33] used a discrete 3D membrane shell dynamic tire model for vehicle ride analysis in the frequency range of 1000 Hz and beyond. Likewise, Ishahara [34] modeled cord-rubber composite components of the tire using a FEM membrane model. Using this approach, the number of DOF in the model is reduced significantly, relative to solid element models, without sacrificing

28

accuracy. Kao [35] developed a FEM tire model with LSDYNA3D and studied the spindle longitudinal and vertical forces during the impact of the tire with semi-circular cleats. His research was extended for six additional impact case studies by Kamoulakos [36] to demonstrate an instability-free algorithm developed in PAMSHOCK. Furthermore, the transient response of the treaded tire to small cleat impacts is analyzed by Cho [37] through an explicit method.

As a summary, finite element models have been developed as a detailed method of representing the tire structure and tire-terrain interaction. The simplified FEM studies use two-dimensional, axisymmetric, and/or coarsely-meshed tire models. These simplifications are either enough for the problem of interest or are due to the limited computational recourses. On the other hand, models that inherit a three dimensional, full FEM, nonlinear, and finely mesh can capture the dynamic response of the tire with high fidelity. Regarding the FEM framework, many researchers used the available FEM packages such as ABAQUS, ANSYS, LS-DYNA, PAM SHOCK, and MARC for modeling and simulation purposes that helps reducing the chance of programming errors. Others, who have developed their own FEM framework, performed code verification techniques, such as stability and convergence checks, to minimize the programming errors. The majority of the studies in the FEM category validated their model's results by comparing them versus experimental measurements.

2.5. Contact and Interaction Modeling Techniques

Once the tire structure and tire material properties are modeled and implemented in an FEM framework, the interface between the model and road surface should be established. This interface searches for the nodal points that are close to the ground (contact search algorithm), and when the contact is detected it applies the required contact condition (contact interface algorithm). Therefore, the contact simulation is initiated by detecting the penetration between the objects and

then, by applying the contact constraints (such as contact forces), this penetration is reduced, minimized, or eliminated.

Two main scenarios in contact problems can be identified as master-slave contact and self-contact. During master-slave contact, surfaces of the two objects have contact with each other, and each node of the slave surface is checked for penetration into the elements of the master surface. The self-contact requires interaction of the segments of the object with themselves, which is the case for crash simulations and airbag deployment. For this type, there is only one slave surface, and nodes/edges of the surface are examined for penetration into the segments of the same surface.

In order to model contact in FEM software, one usually needs to specify the contacting surfaces and type of the contact interface algorithm. The process of contact search algorithm is handled by the software based on the specified model contact interface algorithm, and physics of the problem. The contact search algorithm can be divided into two main methods, node-to-segment correspondence search and node-to-node proximity search. The node-to-node proximity search algorithm looks for the closest master node to a certain slave node, and it is very useful for contact surfaces with matching mesh. Node-to-segment is mostly used for large deformation contact problems that exist between surfaces with non-matching meshes [38]. In this method, the proximity of the slave surface nodes to the master surface segments are examined, and, by preventing the penetration of nodes on the slave surface to corresponding master segments, the non-penetration conditions are enforced [38]), as illustrated in Figure 11.
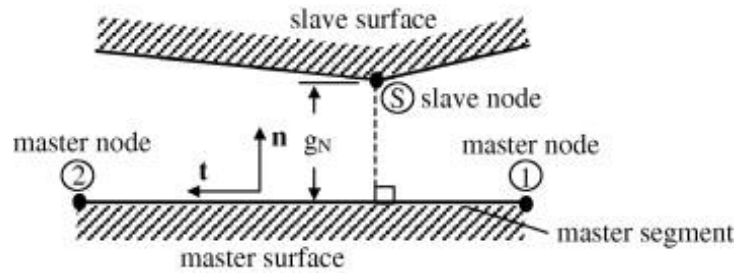
Figure 11: Node-to-segment contact element geometry (Reprinted from The node-to-segment algorithm for 2D frictionless contact: Classical formulation and special cases, Zavarise, G. and L. De Lorenzis, Computer Methods in Applied Mechanics and Engineering, 2009. 198(41–44): p. 3428-3451, Copyright (2014), with permission from Elsevier)

After contact is properly detected, the contact conditions are applied upon penetration using the contact interface algorithm. The two major contact algorithms that are used extensively by FEM codes are Lagrange Multipliers and Penalty Method. Penalty method calculates the contact forces relative to the contact penetration, and no extra degree of freedom is introduced into the system. The amount of penetration is a function of bulk modulus, volume, and surface area of master segment. The penalty parameter is analogous to a spring stiffness that produces a force based on its deflection. Therefore, this method does not consider a zero gap assumption between the contacting surfaces.

The Lagrange Multiplier method adds a term, which consists of a Lagrange Multiplier coefficient and a gap function, to the energy equation of the system. This Lagrange Multiplier coefficient can be interpreted as a reaction force. It should be noted that Lagrange Multiplier introduces new degrees of freedom to the system, which requires additional computational resources. Due to the enhanced accuracy and zero gap feature of the Lagrange Multiplier approach, it is used in this study for defining the contact between tire tread and road surface as well as contact between tire bead and rim. Additionally, for modeling friction behavior between surfaces, the classical Coulomb friction is used.

2.6. Tire Experimental Analysis

In order to validate the model response quantities, the experimental data from Tire Model Performance Test program (TMPT) is used. The TMPT program introduces a standard set of test procedures to evaluate the performance of the tire models in conjunction with multibody system (MBS) vehicle models. These tests are divided into model capability tests and validation tests. The capability tests are designed to study the qualitative behavior of the tire, and show the physical plausibility of using the model. The validation tests contain the experimental test results for some steady-state and dynamic measurements [39]. It should be noted that similar definitions and arrangements for principal axis and force measurements are considered as the basis for constructing the current FEM model.

2.7. Summary

In this literature survey, on-road simulation models that investigated the performance of the wheeled vehicles on non-deformable terrains are reviewed. Models are grouped into three categories, namely: empirical tire methods, physics-based tire methods, and semi-empirical methods. Although, the empirical models are good for simple mobility assessments, they cannot be used outside the conditions under which they are established. The physics-based models incorporate methods including computational physics and numerical analysis to construct an applied framework for the complex problem of soil-tire interaction. These models require high computational resources to handle their highly discretized structures. Additionally, most of the models in this group, except very detailed FEM models, use simplified parameterization procedures to evaluate the material properties and simulation input parameters. Consequently, correlating the physics-based models results with the experimental data is challenging. On the other hand, semi-empirical methods employ the empirical relations in addition to analytical

approaches in order to achieve high fidelity results while keeping the computational effort and number of model variables low. However, in the domains in which these models incorporate the empirical correlations, the limitations of the empirical models exist.

Chapter 3: Tire Material Modeling and Testing

3.1 Introduction

Information about tire material properties, processing, mixing, assembly, and curing are often confidential, and cannot be received from tire companies. Furthermore, the material properties for the same tire from a manufacturer may vary, due to the vulcanization process, for example. The parameterization for individual materials in the tire requires a set of experimental and analytical procedures, such as tension and relaxation length tests, on individual tire sections. Based on this initial analysis, the appropriate material model is chosen and related model coefficients are obtained using data curve fitting. Due to the fact that performing the entire parameterization procedures is out of the scope of this project, the available data from previous studies that conducted for similar tires have been used in the current model [39-44]. It should be

3.2 Tire Structure Components

A modern typical tire is manufactures from nearly 10-35 different components. Different sections of a typical radial passenger car tire are shown in Figure 12. The tire individual parts are created by rubberizing different components including cables, textiles, and steel belts with rubber compounds. These components are assembled on the tire assembly machine into an elastic green tire. Then, tire goes through the vulcanization (curing) process in order to become a unified part. During the curing process, high pressure steam is conducted into the curing pad inside the curing press, and pushes the elastic green tire against the molds. At this stage, the tread pattern and side texts on the tire sidewall are created.
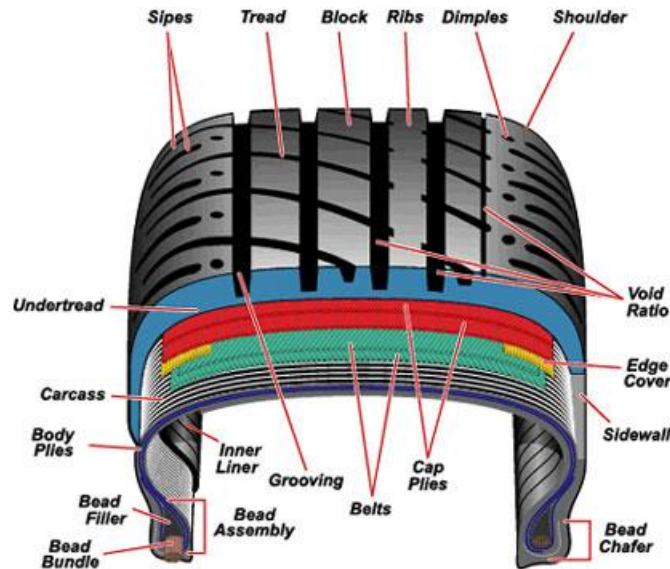
Figure 12: Cross section of a radial passenger car tire

The main tire structural components that significantly contribute to tire structural dynamic and response characteristics are identified as follow:

- The tread is the tire interface with the road. All the forces and moments are generated in this section, so it needs to have certain frictional characteristics. Additionally, it has an approximately homogenous and isotropic structure, which is reinforced with carbon black chains in order to be abrasion resistant. Based on the tire application, tread surface can be smooth (race slick tires) or have a certain pattern.

  The smooth tire has a higher force generation capability on dry surfaces. However, over a wet or icy road, smooth tires cannot produce enough traction, braking, and cornering forces. This is due to the fact that the water film on the road surface does not allow the smooth tire to have a full contact with the road. Therefore, by adding the tread pattern, the water or snow can be disposed more efficiently from the contact patch.

35

- The carcass is a reinforced structure that provides the tire with loading and shock sustainability. It consists of flexible high modulus cords that are embedded into a rubber matrix. The two main carcass structures that are used in the tire industry are bias ply and radial ply tires. The reinforcing cords in bias tires are extended diagonally across the tire, as seen in Figure 13, whereas in radial tires the cords are arranged radially with a crown angle of 90 degree, as shown in Figure 14. The crown angle is defined as the angle between the tire cords and circumferential centerline. The variations in this angle changes the ride comfort and handling properties extensively.

The radial tires allow for a more uniform contact patch pressure distribution during different maneuvers, and consequently have a better performance. Additionally, due the more flexible structure properties of the radial tires, they perform better in enveloping over the bumps and absorbing impact and shock.
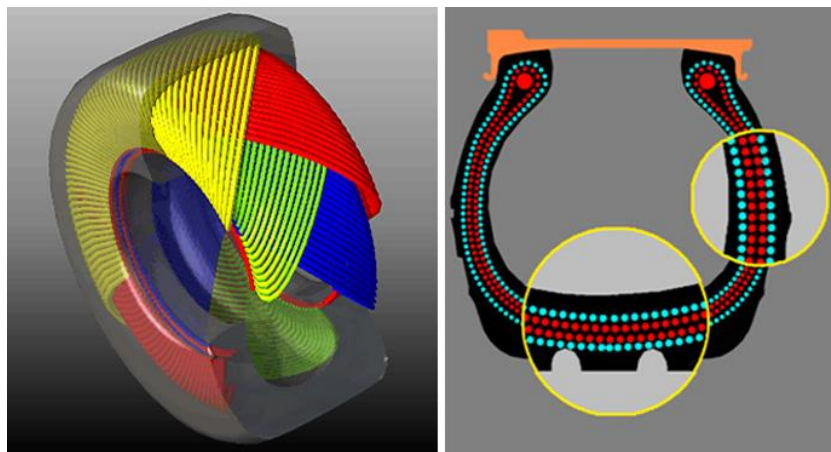
Figure 13: Bias-ply tire structure
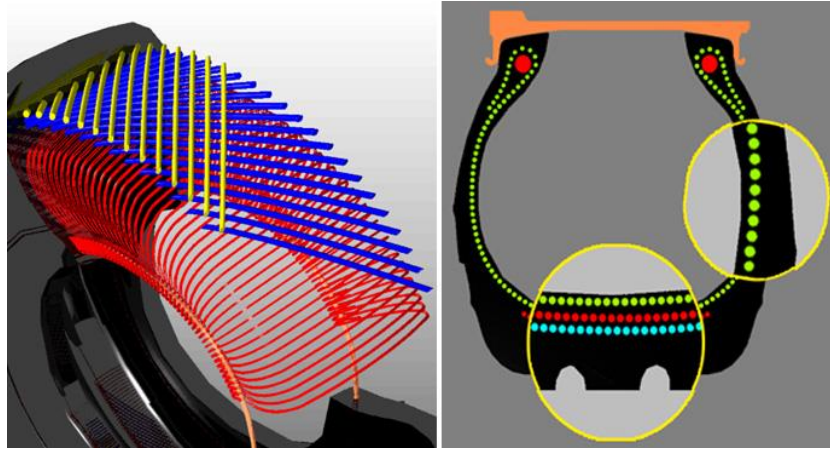
Figure 14: Radial-ply tire structure

- The force transmission between carcass and tread is done by belt elements. These hybrid elements consist of reinforcements elements that are laminated between rubber compounds. Belts limit the deformation of the carcass and provide extra support to the tread elements. Also, belts give an extra resistance toward the puncture to the tire, and help the tire contact patch to remain flat for maximum road contact.

- The interaction between the tire and rim is handled by the bead elements. A bead is a rubber coated high-strength steel cable that gives the strength to the tire in order to sit on the rim. All the forces and moments that are generated in the contact patch are transmitted to the wheel assembly via tire bead elements.

3.3 Tire Structural and Material Properties

The finite element modeling starts with importing the geometrical properties of the system into the software. The cross sectional data from the Tyre Model Performance Test (TMPT) is used for constructing the tire cross-section model in Solid Works, as shown in Figure 15.
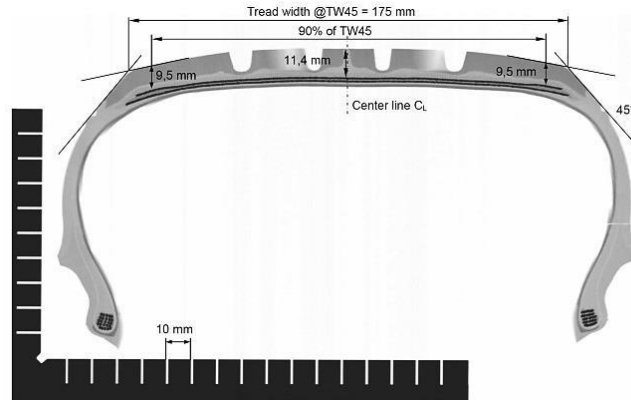
Figure 15: Cross Section of the tire from tire model performance test

In this study, to keep the model relatively simple, the detailed geometrical sections of the tire, such as grooves, and sipes were not considered [45]. Next, the CAD model is transferred to Abaqus/CAE for material assignment and for creating the axisymmetric model from the tire cross-section, as presented in Figure 16. The developed model represents the structure of the actual tire that consists of tread, sidewall, carcass, belt, bead, filler, etc. The sidewall, apex, inner liner, and tread are made of rubber with different properties. Additionally, the carcass, belts, and beads are reinforced composite materials with single or multiple layers of reinforcements [46].
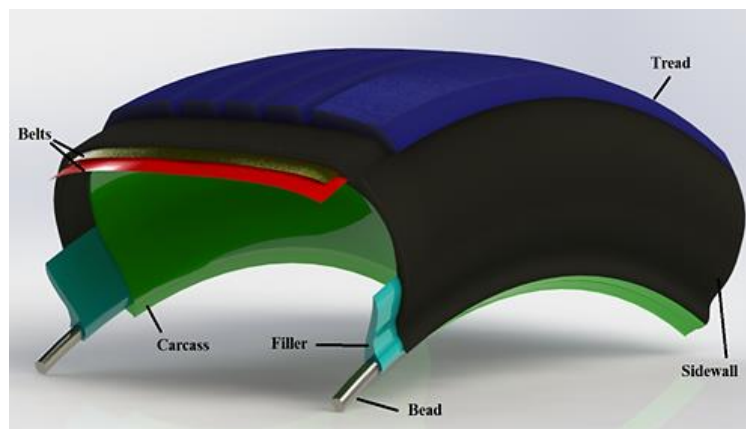
Figure 16: Developed CAD model in Solid Works transferred to ABAQUS for FEM analysis

3.3.1 Hyperelastic material properties

A great portion of the tire structure consists of vulcanized elastomers such as rubber material. Rubber has a nonlinear and incompressible behavior toward loading, which is independent of the strain rate. This behavior is known as hyperelasticity, and the material which shows this behavior is called green elastic material or hyperelastic. A hyperelastic material differs from an elastic material in four main aspects:

- The tire has a high stiffness in the initial step of loading, and dramatically softens in the unloading phase. This phenomenon is known as Mullin's effect.

- Instead of having a hysteresis loop in the stress-strain curves of the loading cycle, the hyperelastic materials have a simple equilibrium curve.

- The hyperelastic materials exhibit different behavior in tension and compression. This is in contrast with the Hooke's law, which considers the stress to be proportional to strain. As a matter of fact, hyperelastic materials such as rubber, have a higher stress magnitude in compression compare to tension for an identical strain magnitude.

- Finally, a hyperelastic material has different modes of deformation that should be studied with respect to the loading conditions that exist in the problem of interest. The deformation modes require corresponding constants in the material model that need to be characterized experimentally. The choice of model constants and required parameterization tests should be done with care in order to avoid false analytical system response quantities that are not presents in the experiments.

The Stress-strain curves for various hyperelastic material models are shown in Figure 17.
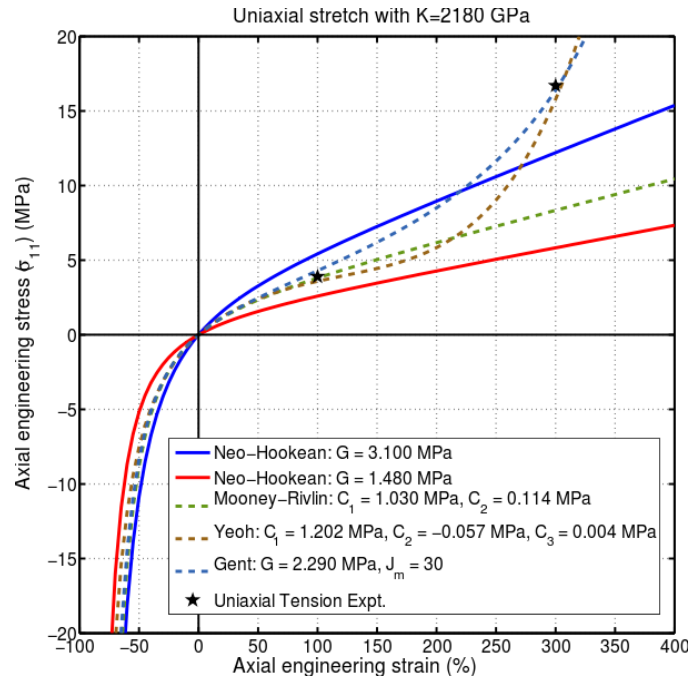
Figure 17: Stress-strain curves for various hyper-elastic materials

3.3.2 Viscoelastic material properties

Viscoelastic materials show a combined elastic and viscous rate dependent behavior when experiencing deformation. In elastic materials, once the applied stress or strain is removed, the specimen quickly returns to its initial condition. On the other hand, viscous materials exhibit a resistance toward the shear flow developed due to the applied stress or strain. In other words, upon applying a constant strain, the material creeps. Similarly, by applying a constant stress, the strain increases and then eventually decreases with time.

The internal damping, rolling resistance, and thermal characteristics of a tire are associated with the viscoelastic property of the rubber. Therefore, in order to accurately quantify the transient response of the tire, the viscoelastic material property should be incorporated. For small strains, the linear viscoelasticity assumption may be chosen. In this case, the relaxation rate of the material is proportional to the immediate stress, and the total viscoelastic behavior can be expressed using

40

the superposition principle. There are different Mechanical models that can describe the viscoelastic characteristics of a material, as presented in Figure 18.
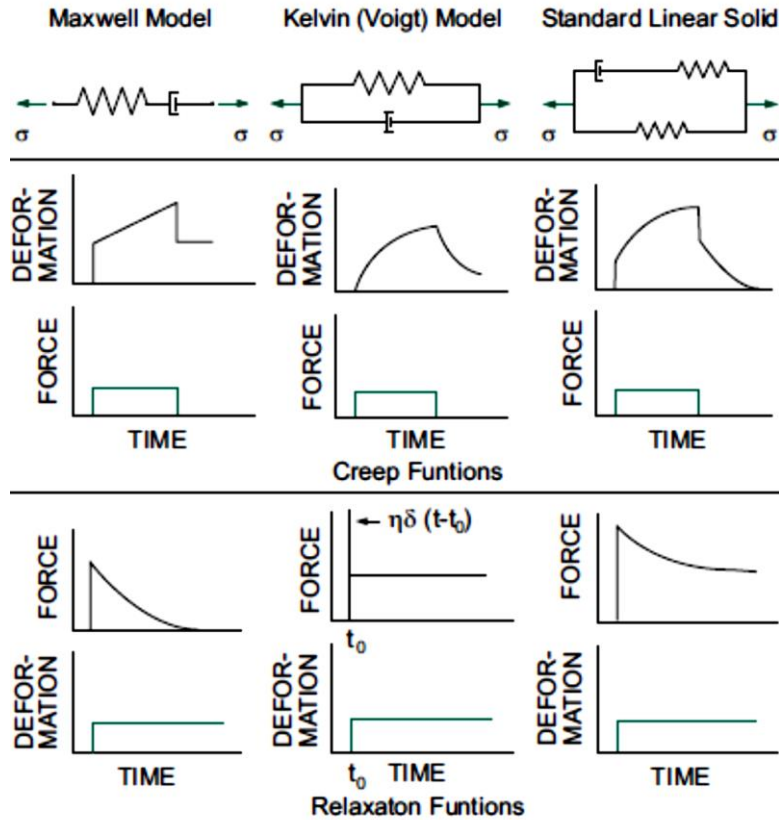
Figure 18: Modeling Mechanical models for describing the viscoelastic behavior

As it can be seen in Figure 18, each of the mechanical models considers a certain form of stress or strain response for the material in different loading conditions. In this study, a more comprehensive material model for expressing the viscoelasticity is used, which is called Generalized Maxwell model. This model is a Prony series representation of stress relaxation functions, and is discussed in 4.3.2 Viscoelastic material modeling.

3.3.3 Reinforcement material (composites) properties

Tire sections such as belts, carcass are classifies as rubber composite materials. These sections include the reinforcement bars that are embedded into a rubber matrix, as seen in Figure 19. These

41

composite materials have an anisotropic behavior, which means that their physical mechanical properties differ with orientation. This composite structure helps the tire section to be flexible while having enough strength to undergo different loading scenarios such as bending, shear, and etc. The ratio of reinforcement modulus to matrix modules for reinforced rubber components is near$10^4 - 10^6$: 1. The high modulus ratio limits the composite deflection due to the inextensibility of cords and incompressibility of the rubber material. During large deformation conditions, this property helps the tire to be flexible and inhibits the frictional sliding between the cords.
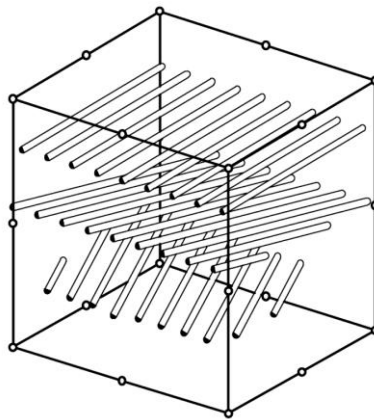
Figure 19: A solid hexahedral FEM element with the reinforcement rebar elements embedded

3.4 Summary

In this section, the tire structure is studied and main structural components that impact the dynamic structural response of the tire are identified. Then, structural properties of the individual components and different material that are used in manufacturing them are studied, and grouped into three main material property families namely: hyperelastic material properties, viscoelastic material properties, and reinforcement material properties. The main features of every material group are studied and proper methods for their modeling and testing are introduced. In the next section, the detailed mathematical framework for characterizing these models and related procedures for parameterizing them are discussed.

Chapter 4: Finite Element Tire Modeling

4.1 Introduction

The main tire structural components and their material properties were studied in Chapter 3. In this chapter, the procedure for developing the full tire FEM model from the geometrical and material properties is discussed. Initially, the geometrical properties of the tire are transformed into the CAD model of the tire section. Then, this model is imported to ABAQUS and the appropriate section properties, and FE elements are assigned.

The individual section features should be defined with proper geometrical properties (e.g., reinforcement spacing, dimensions, angles, etc.) and material properties. The corresponding materials properties are modeled using the available mathematical framework known as material models. The realistic response of the material models are guaranteed by considering the nonlinearities in the model formulation, and parameterizing the model coefficients with experimental data. A simple overview of the process for generating the FEM tire model from the initial data is shown in Figure 20.
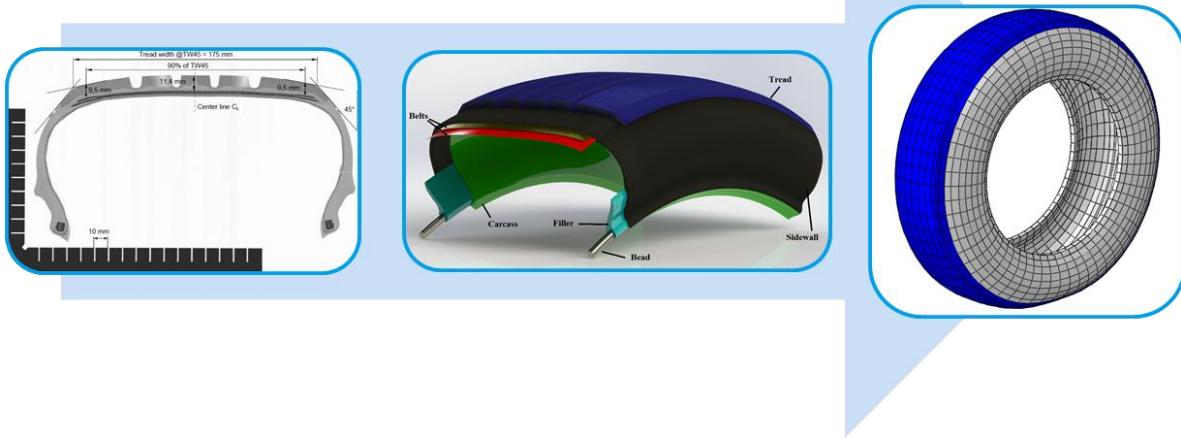
Figure 20: Overview of the process for generating the FEM tire model structure

4.2 Tire Structure and Material Modeling

As mentioned earlier, the modeling procedure starts with the construction of a 2D axisymmetric model based on tire cross-section geometry and material properties. The symmetric feature is used to reduce model size and increase model efficiency. For addressing the circumferential deformation of the tire in the axisymmetric model, hybrid elements with additional twisting degree of freedom (CGAX4H and CGAX3H) are chosen. Also, isotropic material is used for modeling the bead section, which is the main section that is responsible for transmitting tire forces to the rim. Instead of embedding the bead into its surrounding rubber material, the hybrid element CGAX4H is used in the 2D model.

4.3.1 Hyper-elastic Material Modeling

The material models that are used by FE code are usually characterized by the material strain energy functions. These models are usually defined as functions of strain invariants:

$$W = U\ (\overline{I}_1, \overline{I}_2, J) \tag{1}$$

44

Where J is the total volume ratio, and $\bar{I}_1$ and $\bar{I}_2$ are the first and second invariant of the unimodular component of the left Cauchy-Green deformation tensor, and can be identified as [43]:

$$\bar{I}_1 = \bar{\lambda}_1^2 + \bar{\lambda}_2^2 + \bar{\lambda}_3^2 \tag{2}$$

$$\bar{I}_2 = \bar{\lambda}_1^{(-2)} + \bar{\lambda}_2^{(-2)} + \bar{\lambda}_3^{(-2)} \tag{3}$$

The $\bar{\lambda}_\iota$ is the deviatoric stretch that is defined as:

$$\bar{\lambda}_\iota = J^{-\frac{1}{3}}\lambda_i \tag{4}$$

Here J is the total volume ratio and λ_i is the principal stretch that is expressed as:

$$\lambda_i = 1 + \varepsilon_i \tag{5}$$

In which ε_i is the principal strain. It should be noted that in these formulas for incompressible and isothermal materials , $J = 1$ and $\lambda_1\lambda_2\lambda_3 = 1$ [47].

The hyperelasticity was initially modeled by Ronald Rivilin and Melvin Mooney. Their widely-used models are known as Neo-Hookean and Mooney-Rivilin. The rubber components are modeled using Mooney-Rivlin theory of hyperplastic materials, which is based on the rubber strain energy. The strain energy density function with first and second strain invariants can be expressed as follows:

$$W = C_{10} (\bar{I}_1 - 3) + C_{01} (\bar{I}_2 - 3) \tag{6}$$

Where C_{10} and C_{01} are experimentally determined material constants.

In ABAQUS, the hyperplastic elements with reduced integration and hourglassing control are chosen for avoiding shear locking and hourglassing in simulations. The shear locking happens

when a FEM block undergoes bending and consequently cannot follow the curved shape. This makes the strain energy of the element produce shear deformation instead of bending deformation [48]. The reduced integration method which is used for controlling the shear locking suffers from its own numerical difficulty which is called hourglassing. When hourglassing happens, a zero-energy mode is produced in response to bending loading that can propagate when a coarse mesh is used and makes the elements excessively flexible. The numerical values for the hyperelastic material properties used in the model are shown in Table 1.

Table 1: Hyper-elastic properties

Rubber material	C_{10}	C_{01}	Density (kg/m^3)
Tread	805 kPa	1.8 Mpa	1180
Sidewall	170 kPa	845 kPa	1100
Ply	140.32 kPa	390 kPa	1190
Belt	15.33 MPa	20.45 MPa	1200

4.3.2 Viscoelastic material modeling

In order to properly simulate the transient behavior, the tire model with basic hyperplastic property should be enhanced by incorporating viscoelastic property. This property is a function of time and frequency, which can be related to rolling resistance and internal damping of the tire. In this study we consider the time dependency of the viscoelastic property by using a version of the dimensionless relaxation modules expansion, called Prony series:

$$G(t) = G_0 - \sum_{i=1}^{N} G_i\left[1 - e^{(-t/\tau_i)}\right] \tag{7}$$

In this formula G is the elastic shear modulus, and G_0, G_i, τ_i are coefficients that are determined based on curve fitting test data. The viscoelastic properties of the tire rubber component are shown in Table 2.

Table 2: Viscoelastic Properties

Rubber material	Relaxation modulus (g)		Relaxation time (sec)	
Component	G_1	G_2	τ_1	τ_2
Tread	0.1254	0.0921	6.5122	226.7531
Sidewall	0.1597	0.07043	5.9709	243.7300
Ply	0.0934	0.08231	20.8027	350.3403
Belt	0.16832	0.07223	5.9642	204.0324

4.3.3 Reinforcement material modeling

The rubber reinforcement for carcass and belts are superimposed onto the rubber matrices using rebar elements in ABAQUS. Using this approach allows meshing of the cord section independent of the host element. This independent meshing avoids unwanted meshing problems, such as small elements between composite layers. In order to implement the rebar layer, the following information should be specified: rebar thickness, spacing, orientation, location, and material properties. It should be noted that reinforcement materials (steel and nylon wires) are modeled as linear material due to the fact that their strain is negligible relative to the rubber in the inflation and deflection steps.

Table 3: Elastic Property for reinforcements

Reinforcement	Young's modulus (N/m^3)	Poisson's ratio	Density (kg/m^3)
Bead	1.99283 E11	0.31	7490
Ply	5.01275 E9	0.5	1050
Belt	2.17826 E11	0.3	7500
Chaffer	1.725 E9	0.5	940

4.3.4 Material modeling summary

The summary for the process of tire material properties modeling is demonstrated in Figure 21.

Reinforcement Material

The rubber reinforcement for carcass and belts are superimposed onto the rubber matrices using rebar elements in ABAQUS.

Using this approach allows meshing of the cord section independent of the host element.

Reinforcement materials (steel and nylon wires) are modeled as linear materials.

Hyperplastic Property

The rubber components are modeled using Mooney-Rivlin theory.

In ABAQUS, the hyperplastic elements with reduced integration and hourglassing control are chosen for avoiding shear locking and hourglassing in simulations.

Viscoelastic Property

Related to the tire transient behavior

Function of time and frequency , and can be related to rolling resistance and internal damping of the tire.

The time dependency is considered by using a version of the dimensionless relaxation modules expansion, called Prony series.
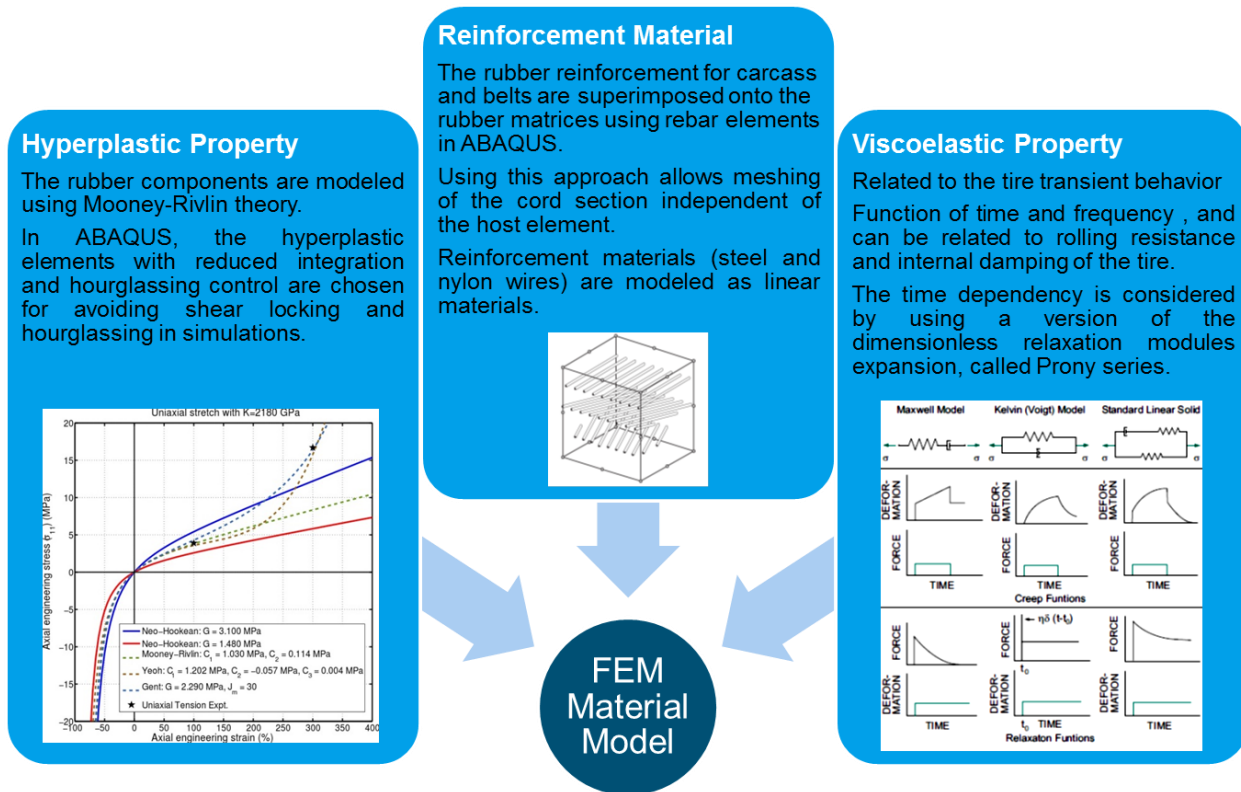
FEM Material Model

Figure 21: Overview of the material modeling steps

48

4.4 FEM Tire Model Assembly

Finally, in order to generate the three-dimensional model of the tire, the symmetric model generation function is used in ABAQUS to transform the 2D model into 3D. As a result of this transformation, all axisymmetric elements CGAX3H and CGAX4G are converted into solid elements C3D8H and C3D6H [49].

4.4.1 Wheel modeling

It should be noted that the rim used for the experimental studies is an aluminum rim that has first mode shapes near 400 Hz. Since this frequency band is far outside of the frequency spectrum in which we analyze the tire, the rim was considered an analytical rigid material during the simulations. Primarily, the uninflated axisymmetric section of the tire is mounted on the rim cross section. The initial width of the uninflated tire is less than the width of the rim, and the tire sits tightly inside the rim. During the inflation step, the pressure boundary condition is kept perpendicular to the deformed geometry of the inner liner to approximate the inflation pressure. During this step, the tire is laterally constrained by the bead seats using the tire-rim contact. The contact model in normal direction is applied using the standard penalty method, and in the tangential direction is applied via the Lagrange Multiplier friction formulation with a 0.45 coefficient of friction. Also, the rim mass and inertial properties are included to be used in dynamic simulations.

4.4.2 Road modeling

In order to simulate tire-terrain interaction, the ground is considered an analytical rigid surface, and a surface-to-surface contact interface is established between tire tread and road in order to avoid the tire tread mesh penetrate the ground. The zero-gap contact is achieved by modeling the contact problem using a Lagrange multiplier method with a combined coefficient of friction of 0.8.

The Lagrange Multiplier method satisfies the contact boundary condition more accurately than other methods, such as the Penalty method [13].

4.5 Summary

The procedure for developing a full finite element tire model from the tire geometrical and material properties are described. This process starts with implementing the geometrical properties of the different tire sections into the ABAQUS software and assigning the proper material models to them. Subsequently, the fully defined section models are modeled using proper FEM elements, and discretized using a structured mesh. Next, all of these individual sections are assembled together to form the completed tire model. Finally, in order to model the interaction of the tire components with each other as well as the tire with the road, proper contact models are assigned to corresponding sections interfaces.

Chapter 5: Finite Element Tire Model Verification and Validation

5.1 Introduction

In order to study the transient behavior of the tire using the developed FEM software, the proper verification and validation exercises should be conducted. Here, verification is the process of evaluating the model implementation to make sure that it does not have any error or programing mistakes. In this regard, the stability and convergence of the model implicit and explicit solvers are examined initially throughout various simulation stages. Furthermore, the system response quantities, such as radial displacements of the elements during static loading and tire natural frequencies are recorded for conducting the order of accuracy test. The order of accuracy test assesses the rate at which the discretization error reduces with systematic mesh refinement.

On the other hand, the validation study is the process of evaluating the extent to which the developed model can represent the real world problem. For this purpose, a series of simulation case studies are considered in order to examine the tire model response characteristics in static and dynamic conditions. Then, the simulation results from these steps are compared to the empirical data from experiments with identical system inputs, and subsequently, accuracy of the developed model is discussed.

5.2 Simulation Case Studies

The finite element analysis of the tire simulations can be categorized as implicit and explicit. The implicit approach uses an iterative approach in addition to Newton-Raphson approximation in order to construct and update the mass and stiffness matrices while enforcing equilibrium at the end of each step. This method is used for solving the preliminary steps in ABAQUS/Standard prior to dynamic transient simulations. These steps consist of mounting the tire on the rim, inflating the

tire, bringing the tire near the ground, performing loading analysis, steady-state rolling, as well as frequency analysis. Using the implicit method at these steps and the ABAQUS results transfer option makes it possible to reach the final transient results more efficiently, due to the fact that it has a quadratic rate of convergence [50]. Moreover, incorporating this method for obtaining the steady-state results, which is the step prior to the transient analysis, makes the computational effort independent of the tire initial condition values, such as inflation pressure and rolling velocity.

For the steady-state simulation, a mixed Eulerian-Lagrangian method is incorporated using the steady-state transport option. The Eulerian coordinate system is used in the rolling direction while the Lagrangian method is used for modeling the material flow through the tire mesh. [51] This method replaces the velocity components in the Lagrangian direction with displacement, which leads to time elimination and having the displacement as an independent field variable.

Next, the transient behavior of the tire in simulations such as traction, braking, and cleat impact was captured using an explicit approach. In this type of analysis, load is applied incrementally to the system. In this case, if the time step is small enough, the system will converge, and the results will be accurate. The drawback of this approach is that it is not time efficient for solving systems that can be solved with implicit methods. Additionally, an explicit method is not suitable for the systems that include cyclic loading. When using the explicit method, a refined mesh is required circumferentially, while for the implicit method the refined mesh is only required in the tire section in contact with the ground. An overview of simulation setup procedure is shown in Figure 22.
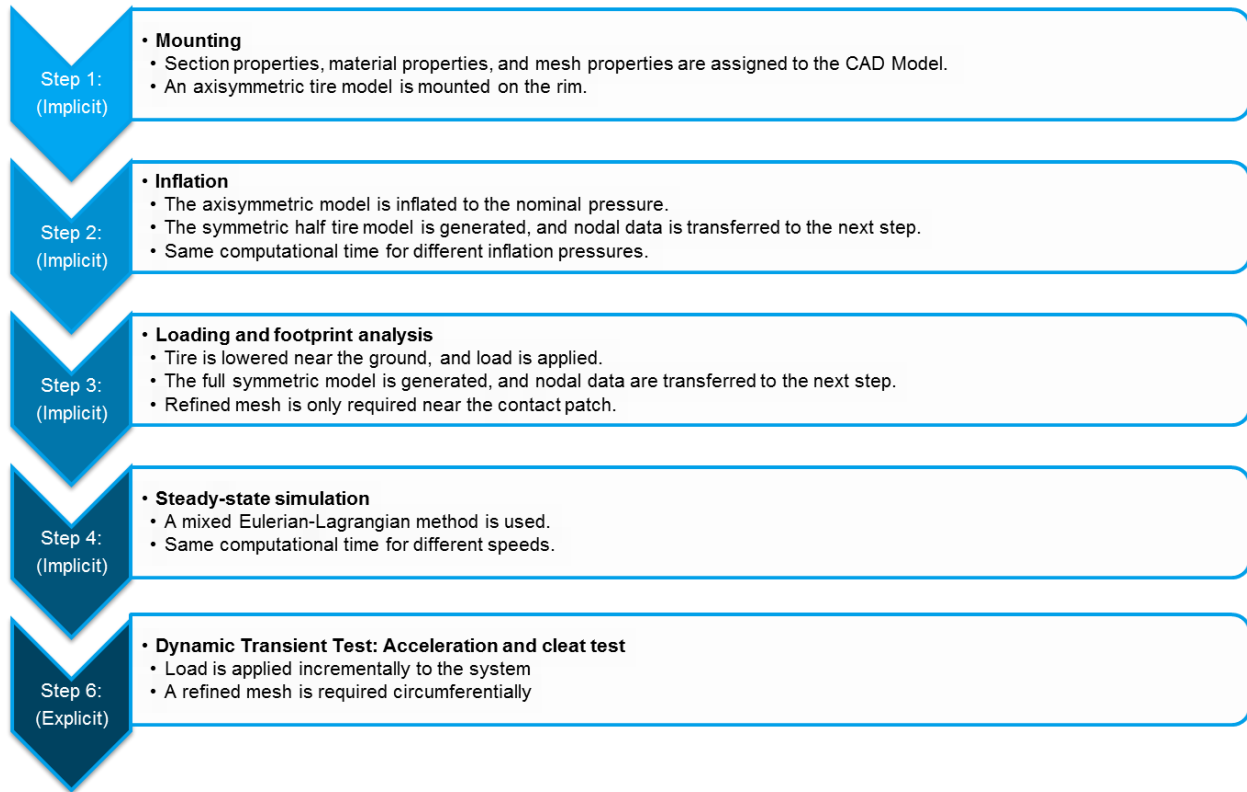
Step 1:
(Implicit)
- **Mounting**
- Section properties, material properties, and mesh properties are assigned to the CAD Model.
- An axisymmetric tire model is mounted on the rim.

Step 2:
(Implicit)
- **Inflation**
- The axisymmetric model is inflated to the nominal pressure.
- The symmetric half tire model is generated, and nodal data is transferred to the next step.
- Same computational time for different inflation pressures.

Step 3:
(Implicit)
- **Loading and footprint analysis**
- Tire is lowered near the ground, and load is applied.
- The full symmetric model is generated, and nodal data are transferred to the next step.
- Refined mesh is only required near the contact patch.

Step 4:
(Implicit)
- **Steady-state simulation**
- A mixed Eulerian-Lagrangian method is used.
- Same computational time for different speeds.

Step 6:
(Explicit)
- **Dynamic Transient Test: Acceleration and cleat test**
- Load is applied incrementally to the system
- A refined mesh is required circumferentially

Figure 22: Simulation setup procedure

5.3 Simulation Case Studies

The following simulations have been performed in this study:

- Static Analysis Test
- Modal Analysis Test
- Dynamic Transient Test: Acceleration and cleat test

These tests have been considered to illustrate the capabilities of the FEM model developed and for its validation.

5.4 Tire Static Analysis

The performance of the proposed method in the early stages of the loading should be verified by experimental results. In this regard, the vertical stiffness of the tire on a flat surface is examined in a quasi-static loading-deflection analysis. During the test, the 100% load index of the tire, which

53

is equal to 5880 N, is applied at the spindle. Next, tire final deflection is measured at three different inflation pressures. The process of loading the tire in the FEM analysis is shown in Figure 23.
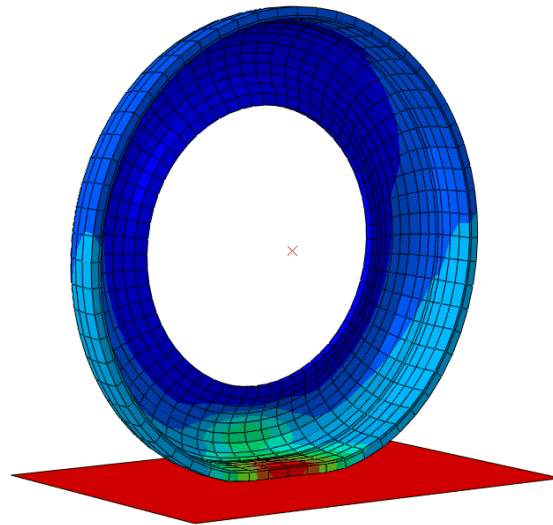

Figure 23: Deflection magnitude contour for the tire during static loading

The results for this analysis are shown in Table 4. It should be noted that the radial stiffness is calculated using the tangent to the interpolated loading-deflection curve at 5880 N.

Table 4: The quasi-static loading deflection test results

Inflation pressure (bar)	Deflection at 100% LI (mm)			Radial stiffness at 100% LI (N/mm)		
	Abaqus	Test	Error	Abaqus	Test	Error
2	29.9	29.2	2.39	216.8	223.5	2.99
2.5	26.5	25.2	5.15	248.6	264.8	6.12
3	23.6	22.1	6.78	280.5	301.6	6.99

Based on the data presented in Table 4, the developed FEM model overestimates the vertical deflection of the tire, and consequently underestimates the vertical stiffness. This phenomenon is further discussed in the following sections. Moreover, due to the nonlinearities in the tire structure, the deviation of the simulation results from the experimental results increases by increasing the tire inflation pressure.

5.5 Tire Modal Analysis

The finite element model is initially compared with steady-state experimental data. In this regard, the modal analysis test is performed in order to extract tire mode shapes and associated natural frequency and damping values. The procedure of performing the modal analysis experiments on the tire is illustrated in Figure 24.
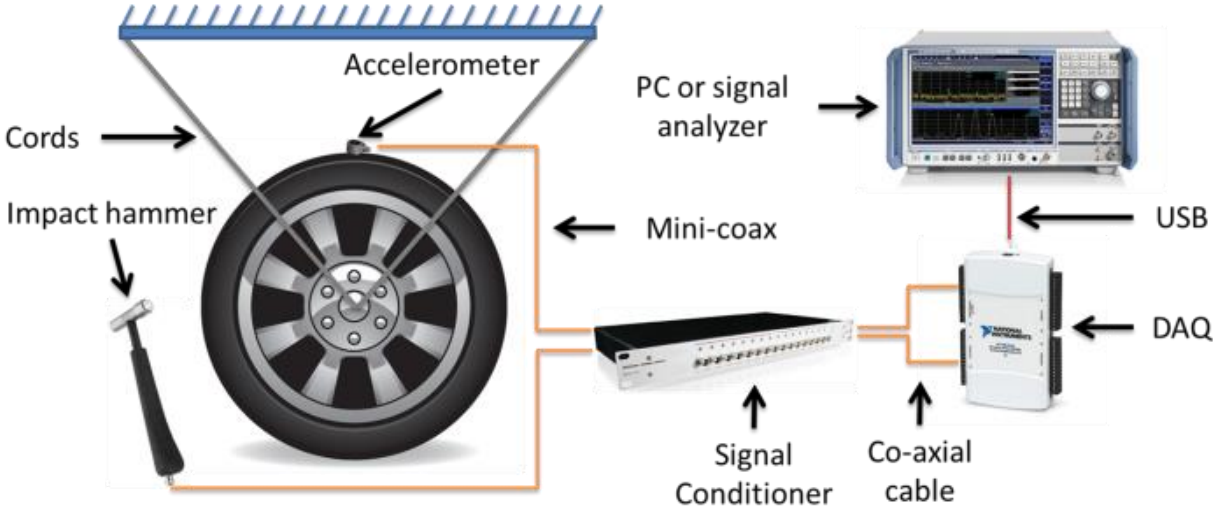
Figure 24: Modal analysis test rig

The modal analysis was conducted using the frequency analysis step in ABAQUS with the Eigensolver set to the Lanczos method. The Lanczos algorithm is a version of power methods that is useful for finding eigenvalues and eigenvectors of large sparse square matrices [52]. This

method handles rigid body modes precisely and is mostly used for complex FEM models that contain different elements, such as solid, shell, and beam.

The sequence for reaching the modal analysis results starts with inflating the tire. In this stage, the nonlinear option was active, which made it possible to perform the linear perturbation at the subsequent step around the nonlinear deformed shape of the tire. For the simulation, the tire was inflated with the pressure of 2.5 bars, and constrained at the hub without any loading.

The data from ABAQUS frequency analysis step is presented in Table 5. The natural frequencies and damping values for the radial modes (R) and transverse modes (T) of the unloaded, non-rotating tire are compared to the experimental values obtained from the TMPT data.

Table 5: Comparison between simulation modal analysis test results and experimental data

Modes	Natural Freq. (Hz)			Damping %		
	ABAQUS	Test	Error	ABAQUS	Test	Error
T0	47.54	47.20	0.72	0.023	0.021	9.52
T1	55.85	61.40	9.04	0.031	0.029	6.9
R0	79.35	81.77	2.96	0.066	0.068	2.94
R1	87.60	97.35	10.01	0.041	0.044	6.82
T2	104.68	116.02	9.77	0.038	0.036	5.56
R2	124.74	122.93	1.47	0.027	0.032	15.63
R3	145.17	149.47	2.87	0.02	0.024	16.67
R4	165.48	176.64	6.31	0.021	0.024	12.5
T3	166.34	179.07	7.10	0.038	0.036	5.56
R5	205.29	205.07	0.10	0.021	0.024	12.5
T4	208.02	217.50	4.35	0.048	0.041	17.07
R6	220.63	235.90	6.47	0.02	0.024	16.67
T5	244.24	246.41	0.89	0.052	0.046	13.04

It can be seen that in most of the modes, the FEM model results correlate with the experimental data within a reasonable error margin. Meanwhile, the model slightly underestimates most of the natural frequencies and radial damping values; on the other hand, it overestimates the transverse damping values. Due to the fact that the frequency analysis was conducted with the nonlinear option active, the estimations error does not show a linear behavior. Moreover, these differences are believed to be a result of the simplifications in the cross-sectional mode shapes (like cross-sectional bending modes), errors in material modeling, lack of treads pattern for the FEM model, and more importantly, the effect of the rim and the boundary conditions. It should also be mentioned that the tire damping grows with an increase in the natural frequency, which makes the tire stiffer in high frequency applications, like ABS braking [53].

The displacement color contour visualization for radial modes is presented in Table 6. Additionally, the transverse mode shapes of the tire are presented in Table 7. For information about the associated natural frequencies and damping values, refer to Table 5. It is worth mentioning that most mode shapes are found to be repeated twice due to the fact that a three dimensional axisymmetric model is used for frequency analysis.
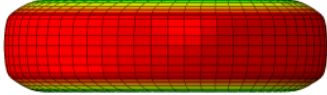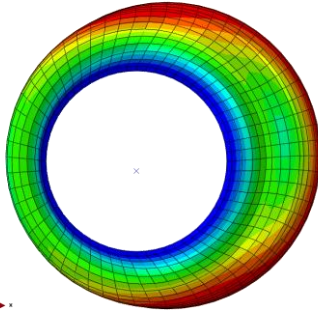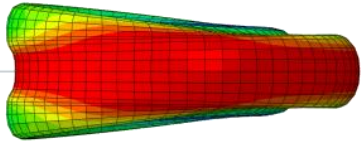
Table 6: Radial modes of the tire
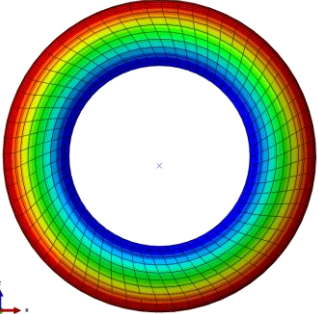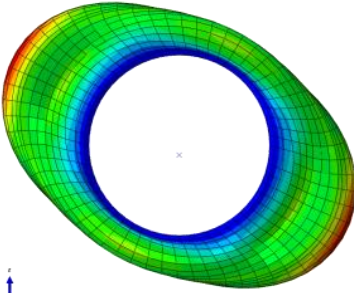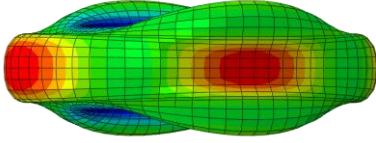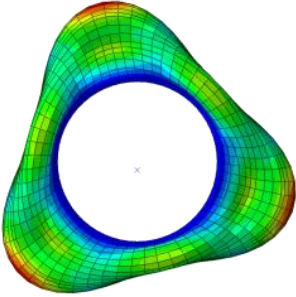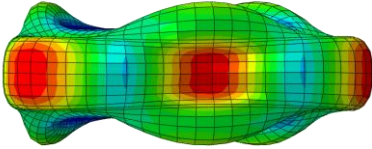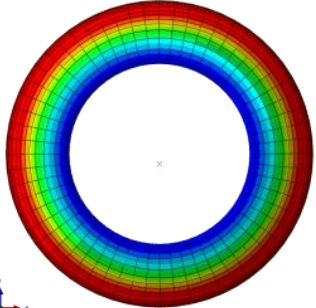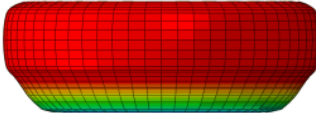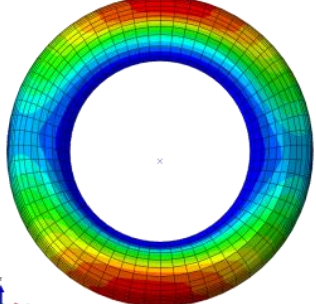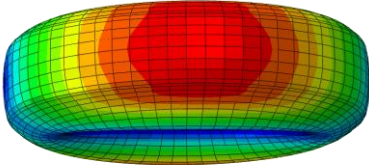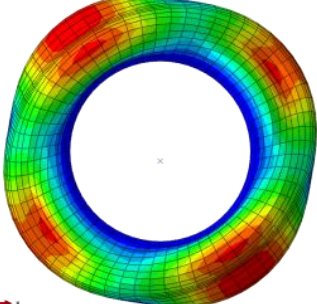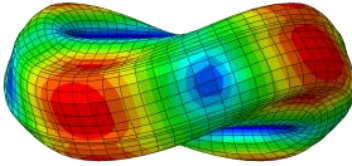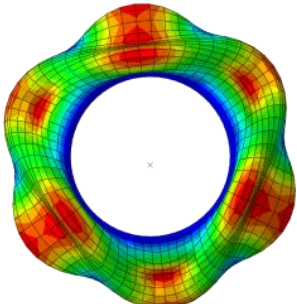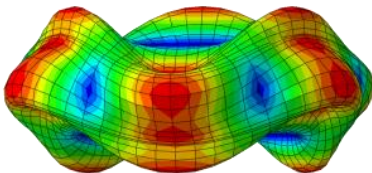
Modes	Front View	Top View
R0		
R1		
R2		
R3		

Table 7: Transverse modes of the tire

Modes	Front View	Top View
T0		
T1		
T2		
T3		

Generally, for mode shapes of the tire which has natural frequencies under 400 Hz, the tire shows modal behavior. In other words, the structural waves in the tire constructively interfere in specific natural frequencies. This trend can be observed in the figures presented in Table 6 and Table 7.

5.6 Dynamic Transient Test

The transient dynamic behavior of the tire was investigated in two case studies: an acceleration test and a cleat test. The sequence of loading starts with mounting the tire on the rim and inflating the tire. It continues with static loading of the tire, and steady-state simulation of the tire for a certain speed. The final state vector of the system at the end of the last step in ABAQUS/Standard will be considered as the initial condition for transient simulations in ABAQUS/Explicit.

5.7 FEM Model Code Verification

For the transient simulations, the accelerating motion of the tire is simulated first, and the stress distribution in the contact patch due to ground forces is studied. Figure 25 shows the color contour of the pressure distribution in the contact patch while the tire (with 5 degree camber) is accelerating with 100 Nm torque applied at its spindle.
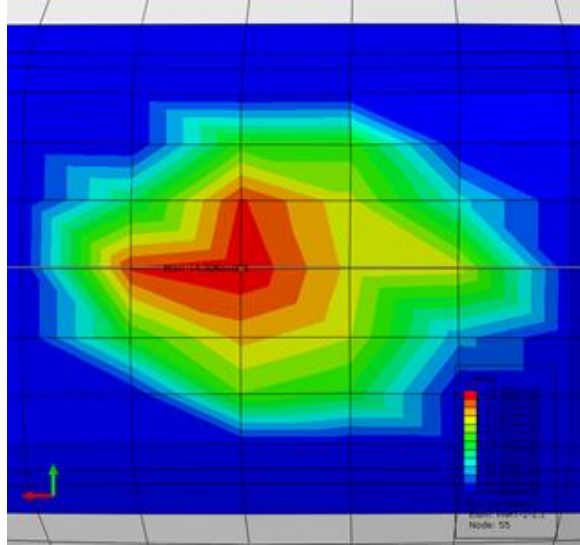
Figure 25: Ground forces in the contact patch during acceleration under 100 N.m torque applied to the rim

Based on the pressure distribution, it can be seen that due to the acceleration, the contact patch area expands, and the peak of the normal ground forces shifts towards the direction of motion, as indicated by the red arrow in Figure 25. Additionally, the 5 degree of camber cause the contact patch not to be symmetric with respect to longitudinal axis.

Similarly, the ground pressure distribution of the tire (without camber) while passing over a rectangular cleat (which has the dimensions of 20 mm width by 40 mm height) at a speed of 10 km/h is shown in Table 8.

Table 8: Ground contact forces in a cleat test for a tire velocity of 10 km/h
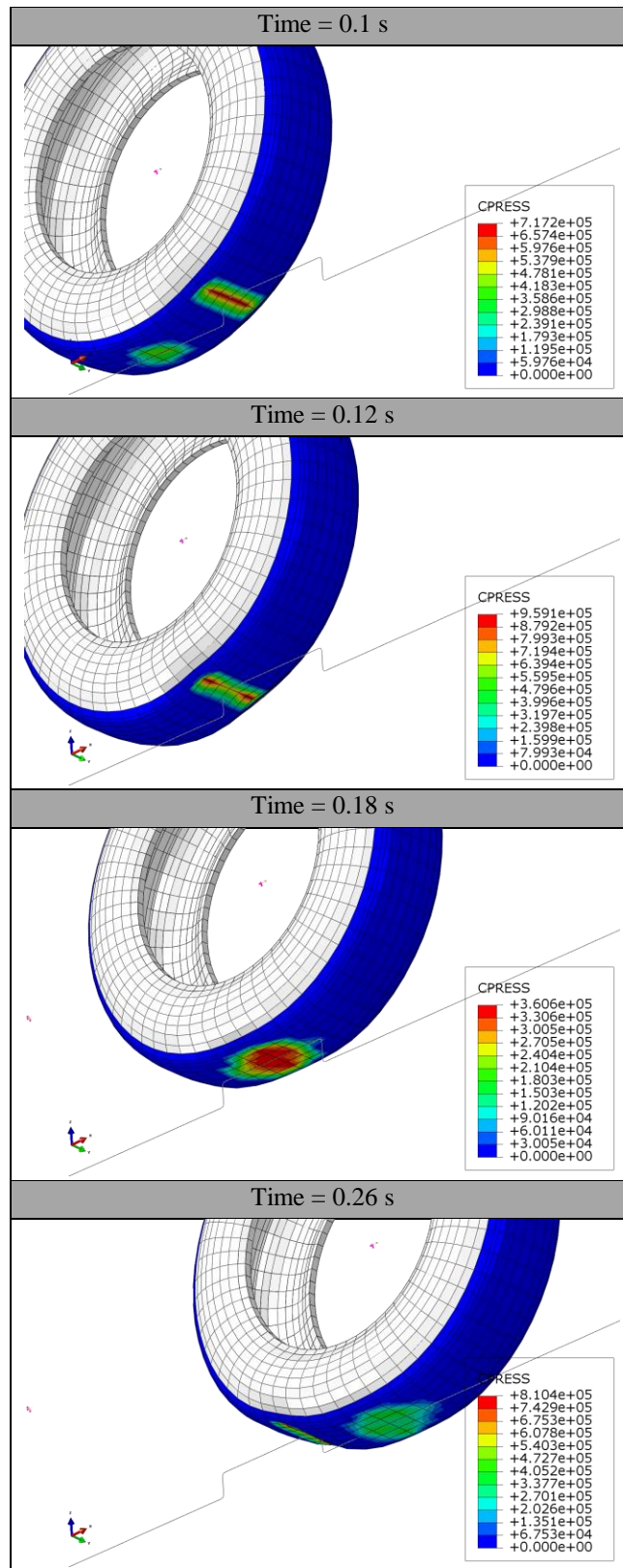
The pressure distribution reaches its maximum when the tire encounters the cleat and the remaining part of the tire loses contact (at t = 0.12 s). For this condition, the tire experiences the critical state of stress at the belt and carcass layer. The tire pressure distribution also shows symmetry with respect to the direction of travel since no camber angle has been applied.

5.8 FEM Model Experimental Validation

For the cleat test simulation represented in Table 8, the vertical displacement of the rim center obtained from the FEM model and the one obtained from experimental testing are shown in Figure 26.
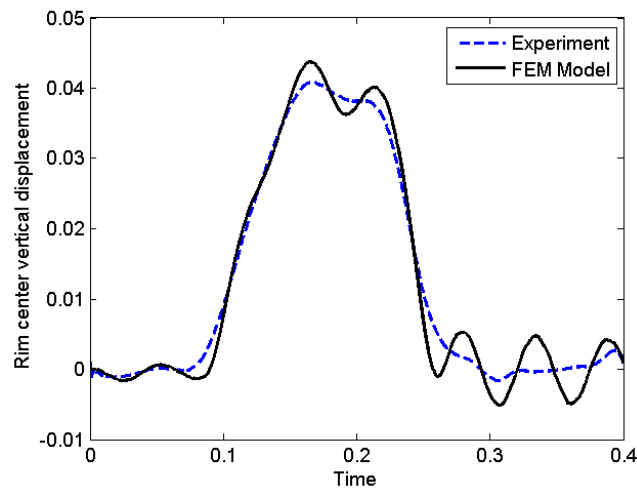
Figure 26: Enveloping characteristics of the tire in a cleat test (cleat size: 20 X 40 mm, pressure: 2 bar, velocity: 10 km/h, normal force: 3000 N)

By comparing the simulation results with experimental data from TMPT it can be observed that the tire vertical displacement during the cleat test shows good agreement with the FEM results. It is worth mentioning that due to the enveloping behavior of the tire and its lengthening of response, the output at the spindle is smoother compare to shape of the obstacle. This was discussed in section 2.42. The FEM model has lower damping values compared to real tire test data. This

behavior was expected from modal analysis, since, as shown in Table 5, the FEM model underestimates the damping values in radial modes, i.e., in-plane excitations.

Due to the discretization of the tire in the circumferential direction and numerical round-off errors, the cleat test simulation results from the FEM analysis contain numerical noise. Consequently, Butterworth filters with appropriate cut-off frequencies are applied to longitudinal and vertical spindle forces. The transient longitudinal and vertical forces at the tire spindle during cleat negotiation are shown in Figure 27 and Figure 28 respectively. In this test, the tire was inflated at 2.5 bar internal pressure, and loaded with a normal dead weight of 3000 N at the spindle. Additionally, it passed over a cleat, which is 10 mm wide and 20 mm tall, at a constant speed of 60 km/h.

Figure 27: Spindle transient longitudinal force during cleat test (cleat size: 10 X 20 mm, pressure: 2.5 bar, velocity: 60 km/h, normal force: 3000 N)
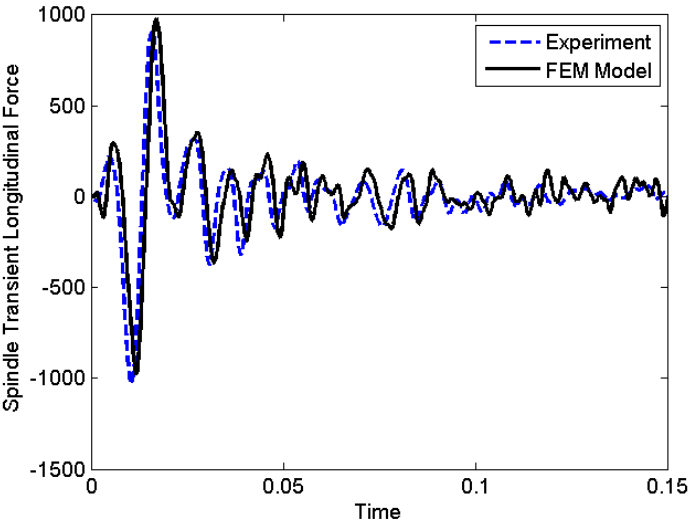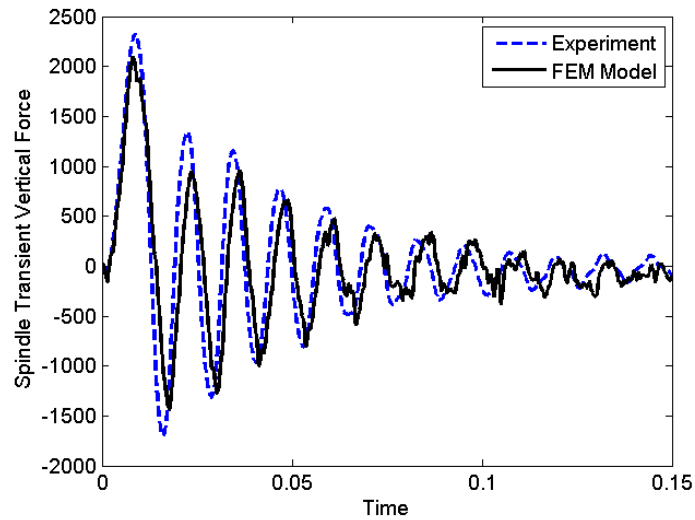
Figure 28: Spindle transient vertical force during cleat test (cleat size: 10 X 20 mm, pressure: 2.5 bar, velocity: 60 km/h, normal force: 3000 N)

In these simulations, data is filtered using a 4th order Butterworth filter with cut-off frequency of 30 Hz for longitudinal force and 55 Hz for normal forces. The cut-off frequency used for spindle forces in vertical direction has a higher value because of higher impact forces and their transient behavior in the vertical direction [54]. One dynamic behavior that can be observed in the vehicle cleat test is the fact that the tire shows a filtering behavior while rolling over the cleat and then it becomes a source of vibration for the vehicle. Furthermore, the fluctuations in the longitudinal force originate in the tire-obstacle impact in addition to the adhesion friction forces in the contact area. As it is shown in Figure 27, the simulation results match the experimental data very well. However, FEM results show some errors in predicting the value and phase shift of the spindle vertical forces. The difference in the peak values is due to the suspension vertical effect during the test, and the phase shift can be associated with the errors in modeling the viscoelastic behavior of the tire.

In order to study the effects of the velocity and normal load on the force characteristics of the tire, another set of experiments were conducted with a reduced speed of 30 km/h and three vertical

65

loading conditions. The cleat size and internal tire pressure were kept constant for these case studies. The longitudinal and vertical forces at the rim center during the cleat test are shown in Figure 29 and Figure 30.
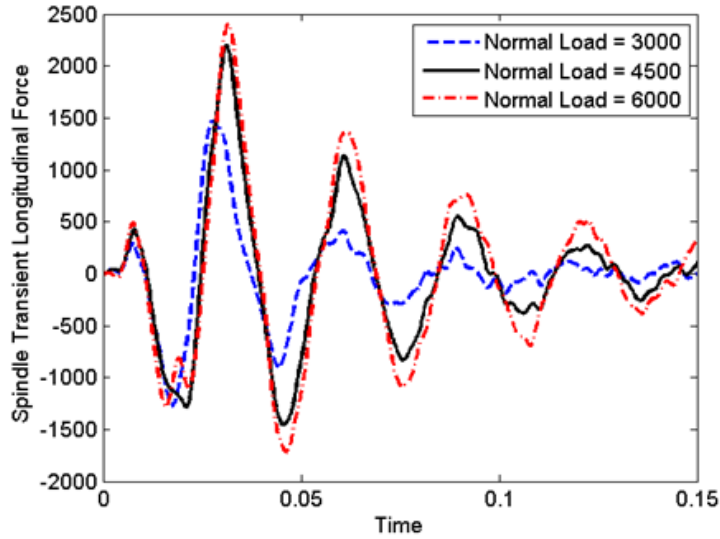

Figure 29: Effect of the loading on spindle transient longitudinal force during cleat test (cleat size: 10 X 20 mm, pressure: 2.5 bar, velocity: 30 km/h)
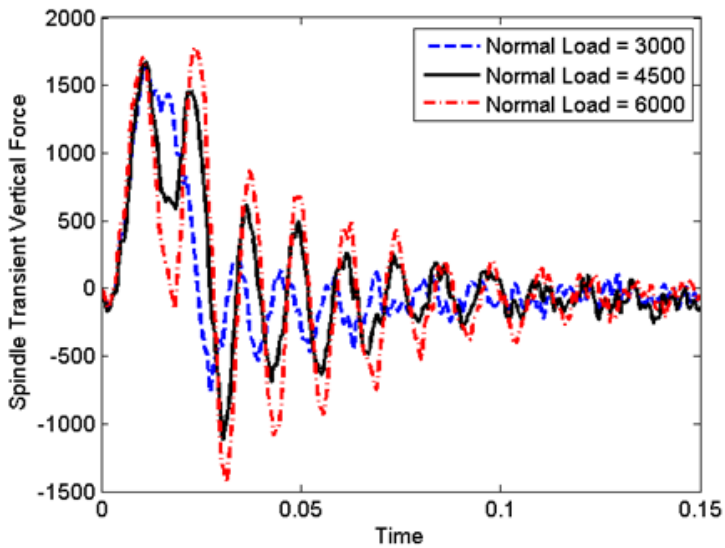

Figure 30: Effect of the loading on spindle transient vertical force during cleat test (cleat size: 10 X 20 mm, pressure: 2.5 bar, velocity: 30 km/h)

As shown in Figure 29, the peak of the spindle force increases with an increase in the normal force. The changes in the peak values show the dependency of the tire stiffness to normal load. Furthermore, it was observed that the horizontal shift in force plots, which is a representation of the relaxation length, does not change significantly with changes in the longitudinal speed. This could be interpreted as the reason for which the tire dynamic response is autonomous (time independent) and it only depends on the displacement. Comparing the Figure 27 and Figure 29 also shows that increasing the tire speed, while keeping the normal load constant, can attenuate the first peak of the longitudinal force. The same behavior is also observed by other studies [55]. This could be due to the fact that with increasing the speed, tire forehead will envelope faster over the obstacle, which induces less longitudinal deflection during the first contact.

Furthermore, it can be observed that, by increasing the vertical load, and consequently expanding the contact patch, the first peak of the vertical force occurs earlier. Also, one interesting behavior happens after the first peak of the vertical load, which is a sudden drop in the vertical force while increasing the normal load. This phenomenon happens as a result of reduced stiffness at the center of contact patch [56].

5.9 Summary

The integrity and accuracy of the developed FEM model is evaluated through a set of code verification and model validation case studies. In the code verifications tests, it is ensured that the numerical algorithms are consistent and convergent, and no coding mistake is present in the software. Next, the model validation experiments are conducted in a series of tests from design of experiment table, which range from quasi-static to modal analysis and transient analysis tests. After assessing the model accuracy by comparing it with experimental data within its domain of validation, the interpolation or extrapolation of the model to the intended future uses can be done.

Chapter 6: Conclusion and Future Work

6.1 Conclusion

A three dimensional finite element tire model is proposed for estimating the behavior of a pneumatic tire during dynamic simulations. The model was developed in ABAQUS software based on the geometrical and material properties of a Michelin tire from the Tyre Model Performance Test (TMPT). The model is validated in two stages. First, a series of frequency analysis tests are conducted on the tire to extract mode shapes, natural frequencies, and damping values. Based on the available experimental results, it can be stated that the model follows the experimental results within an acceptable error margin for most of the modes. It was observed that the FEM model slightly underestimates most of the natural frequencies and radial damping values, and overestimates the transverse damping values. These differences are considered to be results of simplifications in the cross-sectional shapes, errors in material modeling, lack of tread pattern for the FEM model, and the effect of the rim and boundary conditions.

In order to study the transient characteristics of the tire, a series of dynamic simulations including acceleration maneuver and cleat impact are conducted. During the acceleration test, torque is applied to a tire with camber, and ground pressure distribution was studied. Next, the cleat tests are performed for different cleat sizes, normal loads, and tire longitudinal velocities, and results are validated using the experimental data. It should be noted that, due to the discretization effect and numerical noise in FEM results, they are filtered using discrete filters with appropriate cut-off frequencies. Furthermore, the effects of changing individual parameters on the spindle vertical and longitudinal forces are discussed.

The results showed that the developed model can predict the longitudinal force characteristics with a good match. There is a small error in evaluating the normal force at the tire spindle which could be associated with the suspension effects and uncertainties in specifying the viscoelastic material properties. Moreover, it was shown that the tire general dynamic response is autonomous (time independent) and it only depends on the displacement. As a proposition for the future tire dynamic studies, it is suggested that the tire FEM model is integrated into a MBS car model in order to include the effect of the suspension in the tire transient force characteristics.

6.2 Future Work

The following aspects are suggested to be incorporated for the future investigations in order to explore the integrity and the application potentials of the proposed concepts in this study:

6.2.1 FEM tire modeling future work

- An automated software framework can be established for importing the tire section geometrical properties, and generating the required axis-symmetric or full symmetric tire CAD models. Using this method, the sensitivity of the system response quantities to the tire geometry variations and uncertainties can be examined. Also, it can be used for transforming the future tire designs into the FEM tire models more efficient.

- The effect of using different material models and finite element types on the accuracy of the model results can be investigated.

- The FEM tire model can be enhanced with thermal elements in order to study the related effects on the stress distribution, and force characteristics of the tire during transient high frequency applications such as ABS braking.

69

6.2.2 Experimental future work

- The anisotropic tire sections such as belts and carcass needs to be further analyzed quantitatively. A more rigorous experimental material testing and modeling is suggested for obtaining the reliable estimate.

- The effect of the tread elements in transient response of the tire need be identified. It is recommended that similar simulations, such as ones conducted in this research, are performed on both treaded and buffed tires and results are compared with corresponding FEM models.

References

1. Gipser, M., *FTire - the tire simulation model for all applications related to vehicle dynamics.* Vehicle System Dynamics, 2007. **45**: p. 139-151.
2. Rao, K.N., et al., *A study of the relationship between Magic Formula coefficients and tyre design attributes through finite element analysis.* Vehicle System Dynamics, 2006. **44**(1): p. 33-63.
3. Korunović, N., et al., *Finite Element Analysis of a Tire Steady Rolling on the Drum and Comparison with Experiment*. 2011. Vol. 57. 2011.
4. Wong, J.Y., *Theory of Ground Vehicles*. 4th ed. 2008, Hoboken, NJ: John Wiley & Sons.
5. French, T., *Construction and Behaviour Characteristics of Tyres*. 1959: Institution of Mechanical Engineers, Automobile Division, London, England.
6. HC, V. and H. PACEJKA, *TIRE AS A VEHICLE COMPONENT.* NATIONAL BUREAU OF STANDARDS MONOGRAPHS, 1971(M 122): p. 545-&.
7. Segel, L., et al. *The mechanics of heavy-duty trucks and truck combinations*. 1981. Michigan University, Ann Arbor, Engineering Summer Conferences.
8. Kern, W. and S. Futamura, *Effect of tread polymer structure on tyre performance.* Polymer, 1988. **29**(10): p. 1801-1806.
9. Engineers, S.o.A., *Vehicle Dynamics Terminology*. 2008.
10. Jazar, R.N., *Vehicle dynamics: theory and application*. 2008: Springer.
11. Pacejka, H.B., and Bakker, E., *The Magic Formula Tyre Model.* Vehicle System Dynamics, 1992. **21**(001): p. 1-18.
12. Oertel, C., *On Modeling Contact and Friction Calculation of Tyre Response on Uneven Roads.* Vehicle System Dynamics, 1997. **27**(S1): p. 289-302.
13. Chae, S., *Nonlinear Finite Element Modeling and Analysis of a Truck Tire*, in *Intercollege Graduate Program in Materials*. 2006, Pennsylvania State University. p. 207.
14. Mastinu, G. and E. Pairana, *Parameter Identification and Validation of a Pneumatic Tyre Model.* Vehicle System Dynamics, 1992. **21**(sup001): p. 58-81.
15. Oertel, C., and Fandre, A. *Ride Comfort Simulations and Steps Towards Life Time Calculations: RMOD-K and ADAMS*. in *International ADAMS User's Conference*. 1999. Berlin, Germany.
16. Gallrein, A., and Backer, M. , *CDTire: a tire model for comfort and durability applications.* Vehicle System Dynamics, 2007. **45**(1): p. 69-77.
17. Haney, P., *The Racing & High-Performance Tire*, in *Sports Car magazine*. 2004.
18. Lidner, L., *Experience with the magic formula tyre model.* Vehicle System Dynamics, 1992. **21**(S1): p. 30-46.
19. Apetaur, M., *Modelling of transient nonlinear tyre responses.* Vehicle System Dynamics, 1992. **21**(S1): p. 116-126.
20. Kilner, J., *Pneumatic tire model for aircraft simulation.* Journal of Aircraft, 1982. **19**(10): p. 851-857.
21. Guo, K., *Tire roller contact model for simulation of vehicle vibration input*. 1993, SAE Technical Paper.
22. Misun, V., *Road loads when a vehicle moves over an unevenness in a road.* International Journal of Heavy Vehicle Systems, 1994. **1**(4): p. 417-432.
23. Badalamenti, J. and G. Doyle, *Radial-interradial spring tire models.* Journal of Vibration, Acoustics Stress and Reliability in Design, 1988. **110**(1): p. 70-75.

24. Gillespie, T.D., *Fundamentals of vehicle dynamics.* Training, 1992. **2005**: p. 12-15.

25. Eichler, M., *A ride comfort tyre model for vibration analysis in full vehicle simulations.* Vehicle System Dynamics, 1997. **27**(S1): p. 109-122.

26. Loo, M., *A model analysis of tire behavior under vertical loading and straight-line free rolling.* Tire Science and Technology, 1985. **13**(2): p. 67-90.

27. Padovan, J. *Numerical simulation of rolling tires*. in *Tire rolling losses and fuel economy, An R&D Planning Workshop*. 1977.

28. Trivisonno, N., *Applications of Tire Thermography to Rolling Resistance.* Tire rolling losses and fuel economy, 1977: p. 19-20.

29. Noor, A.K., C.M. Andersen, and J.A. Tanner, *Exploiting symmetries in the modeling and analysis of tires.* Computer Methods in Applied Mechanics and Engineering, 1987. **63**(1): p. 37-81.

30. Mousseau, C. and G. Hulbert, *An efficient tire model for the analysis of spindle forces produced by a tire impacting large obstacles.* Computer methods in applied mechanics and engineering, 1996. **135**(1): p. 15-34.

31. Zaghloul, S. and T. White, *Use of a three-dimensional, dynamic finite element program for analysis of flexible pavement.* Transportation Research Record, 1993(1388).

32. Scavuzzo, R.W., T.R. Richards, and L. Charek, *Tire vibration modes and effects on vehicle ride quality.* Tire Science and Technology, 1993. **21**(1): p. 23-39.

33. ZACHOW, D., *3D membrane shell model in application of a tractor and PKW tyre.* Vehicle System Dynamics, 1997. **27**(S1): p. 163-172.

34. Ishihara, K., *Development of A Three-Dimensional Membrane Element for the Finite Element Analysis of Tires.* Tire Science and Technology, 1991. **19**(1): p. 23-36.

35. Kao, B. and M. Muthukrishnan, *Tire transient analysis with an explicit finite element program.* Tire Science and Technology, 1997. **25**(4): p. 230-244.

36. Kamoulakos, A. and B. Kao, *Transient dynamics of a tire rolling over small obstacles-a finite element approach with PAM-SHOCK.* Tire Science and Technology, 1998. **26**(2): p. 84-108.

37. Cho, J.R., et al., *Transient dynamic response analysis of 3-D patterned tire rolling over cleat.* European Journal of Mechanics - A/Solids, 2005. **24**(3): p. 519-531.

38. Zavarise, G. and L. De Lorenzis, *The node-to-segment algorithm for 2D frictionless contact: Classical formulation and special cases.* Computer Methods in Applied Mechanics and Engineering, 2009. **198**(41–44): p. 3428-3451.

39. Lugner, P. and M. Plöchl, *Tyre model performance test: First experiences and results.* Vehicle System Dynamics, 2005. **43**(sup1): p. 48-62.

40. BARANOWSKI, P., et al., *Assessment of Mechanical Properties of Offroad Vehicle Tire: Coupons Testing and FE Model Development.* acta mechanica et automatica, 2012. **6**(2).

41. *Tyre Model Performance Test Continental Data Description* 2003. p. 9.

42. Lugner, P. and M. Plochl, *Tyre model performance test: first experiences and results.* Vehicle System Dynamics, 2005. **43**: p. 48-62.

43. Ghosh, P., et al., *Material property characterization for finite element analysis of tires.* Rubber World, 2006. **233**(4): p. 22.

44. Cho, J., H. Jeong, and W. Yoo, *Multi-objective optimization of tire carcass contours using a systematic aspiration-level adjustment procedure.* Computational mechanics, 2002. **29**(6): p. 498-509.

45. Cho, J.R., et al., *Mesh generation considering detailed tread blocks for reliable 3D tire analysis.* Advances in Engineering Software, 2004. **35**(2): p. 105-113.

46. cheng, G., et al., *Influence of Camber Angle on Rolling Radial Tire under Braking State.* Procedia Engineering, 2011. **15**(0): p. 4310-4315.

47. Yang, X., O. Olatunbosun, and E.O. Bolarinwa, *Materials Testing for Finite Element Tire Model.* Society of Automotive Engineers, 2010.

48. Sun, E.Q., *Shear Locking and Hourglassing in MSC NAstran, ABAQUS, and ANSYS*, in *MSC.Software's Virtual Product Development Conferences*. 2006, MSC Software.

49. Surendranath, H., *Applying FEA to tire design: an integrated approach for transient rolling of tires*. 2005, SIMULIA.

50. Hibbit, Karlsson, and Sorensen, *ABAQUS/Standard Analysis User's Manual*. 2007: Hibbit, Karlsson, Sorensen Inc.

51. Synka, J. and A. Kainz, *A novel mixed Eulerian–Lagrangian finite-element method for steady-state hot rolling processes.* International Journal of Mechanical Sciences, 2003. **45**(12): p. 2043-2060.

52. Cullum, J.K. and R.A. Willoughby, *Lanczos Algorithms for Large Symmetric Eigenvalue Computations, Vol. 1*. 2002: Society for Industrial and Applied Mathematics. 273.

53. Kindt, P., P. Sas, and W. Desmet. *Three-dimensional Ring Model for the Prediction of the Tyre Structural Dynamic Behaviour*. in *ISMA*. 2008.

54. Balaramakrishna, N. and R.K. Kumar, *A study on the estimation of SWIFT model parameters by finite element analysis.* J Automobile Eng, 2009. **223**(10): p. 1283-1300.

55. Gipser, M., *FTire, a New Fast Tire Model for Ride Comfort Simulations*. Esslingen University of Applied Sciences: Munich.

56. Schmeitz, A.J.C., *A Semi-Empirical Three-Dimensional Model of the Pneumatic Tyre Rolling over Arbitrarily Uneven Road Surfaces*, in *Mechanical Maritime and Materials Engineering*. 2004, Delft University of Technology Netherlands.